

**Final Report**  
**Phase III - Chevron Special Concentrically Braced Frames**  
**with Beam Yielding**

**Parametric Investigations using Nonlinear Analysis**

**by**

Charles Roeder, Dawn Lehman and Jeffrey Berman  
University of Washington

Qiyang Tan  
Visiting Graduate Student at the University of Washington

Hayato Asada  
Visiting Assistant Professor from Kobe University

Andrew Sen  
Post-Doctoral Appointment at the University of Washington

**A Research Report to the American Institute of Steel Construction**

September 11, 2019

## Table of Contents

Table of Contents	ii
List of Figures	iv
List of Tables	v
Abstract	vi
Chapter 1 Introduction	1
1.1 Background	1
1.2 Current Codes and Research	3
1.3 A Comprehensive Research Study	7
Chapter 2 – Summary of Phase I and II Research	8
2.1 Summary of Phase I	8
2.2 Summary of Phase II	9
2.3 Observations and Conclusions	10
2.3 Recommendations	12
Chapter 3 – Overview of Modeling Approach and Parametric Study	13
3.1 Goals and Scope of Parameter Study	13
3.2 Construction and Verification of the Computer Model	14
3.3 Adaptation of the Computer Model to Parameter Study	20
3.4 Scope of Analyses	23
Chapter 4 – Analytical Results	25
4.1 Parameter Study Analysis	25
4.2 Seismic Response-History Analysis of 3 and 9-Story Chevron SCBFs	34
Chapter 5 Detailed Analysis of Parameter Study Results	41

5.1 Global Brace Slenderness Ratio	41
5.3 Effect on Column Axial Force	44
5.4 Axial Force on the Beam	44
5.5 Effect of Different Beam-Column Connections and Beam-Column Strength Ratio	45
5.6 Beam Deflections	46
Chapter 6 Summary and Conclusions	47
6.1 Summary	47
6.2 Conclusions	48
6.3 Further Issues	49
References	50

## List of Figures

Figure 1-1. Comparison of braced frame behavior: (a) chevron frame with a yielding beam, and (b) X-braced SCBF on the bottom two stories and a chevron with a strong beam on top story.....	4
Figure 1-2. Test results on a chevron frame with a yielding beam from Okazaki (2013) .....	5
Figure 3-1. Three-Story Test Frame.....	15
Figure 3-2. Analytical Model: (a) Finite Element Mesh and (b) Loading and Boundary.....	15
Figure 3-3. Computed Results: (a) Model with slab and (b) Model without slab.....	16
Figure 3-4. Schematic layout of fibers for HSS and wide flange cross sections.....	17
Figure 3-5. Rotational connection model of corner connections (Hsiao et al., 2012). .....	18
Figure 3-6. Comparison of OpenSees Model and Test Results .....	20
Figure 3-7. Computed Response of the Baseline Structure .....	22
Figure 4-1. Three-story and nine-story archetype SCBFs: (a) three-story and (b) nine-story buildings .....	35
Figure 4-2. Target UHS spectra and scaled spectra of the selected ground motion suites for: (a) three-story buildings, and (b) nine-story buildings.....	37
Figure 4-3 Maximum drift on each story for all buildings for the 2% in 50 year hazard level: (a) 3 story proposed chevron; (b) 3 story AISC chevron; (c) 3 story X-braced d) 9 story proposed chevron; e) 9 story AISC chevron f) 9 story X-braced.....	38
Figure 4-4. Percentage of ground motions causing selected damages states: (a) 3 story 2% in 50-year hazard, b) 9 story 2% in 50-year hazard. ....	40
Figure 5-1. Story Shear vs. Story Drift for most heavily damaged level.....	42
Figure 5-3. Effect of $b/t$ ratio on deformation capacity prior to brace fracture.....	43
Figure 5-4. Beam geometry and plastic mechanisms: (a) chevron beam restrained with corner gusset plates, (b) and (c) chevron beam restrained without corner gusset plate and having simple shear connections for middle or top story respectively. ....	44
Figure 5-5. Normalized maximum beam deflections at 2% story drift .....	46

## List of Tables

Table 4-1. Summary of Parameter Analysis Results.....	26
Table 4-2. Three-story archetype member sizes .....	35
Table 4-3. Nine-story archetype member sizes .....	36

## Abstract

Design of chevron-configured special concentrically braced frames requires beams strong enough to remain elastic under idealized forces, where the tension brace sustains its full capacity and the compressive brace is either at 100% or 30% of its compressive capacity ( $P_{cr}$ ). These requirements result in large, deep and stiff beams, which has resulted in a reduction in the use of SCBFs, with engineers preferring BRBs or other systems, including reinforced concrete shear walls. A recent AISC-sponsored project has investigated a new approach to designing these systems that includes a secondary yield mechanism of beam yielding. The research project tested six (6) one-story frames and one (1) three-story frame to investigate the impact of beam yielding on the seismic performance with a focus on the development of yield mechanisms and failure modes and drift-range capacity. Test variables included beam strength, beam stiffness and beam-to-column connection restraint. The results indicate that beam yielding increases the drift capacity of SCBFs while maintaining the design strength. However, beams must have adequate resistance to develop the full resistance of the braces prior to buckling and this requirement must be part of the design. Based on recommendations from the advisory panel, an additional nonlinear analytical study was performed to extend the experimental research studying the impacts of various design parameters outside the tested range and is reported on here. The study used experimentally validated numerical modeling to investigate parameters that were addressed in the experiments, specifically: (1) beam strength with a focus on the axial stress ratio induced by the brace unbalanced forces, (2) brace seismic compactness ratio and  $KL/r$  ratio, (3) brace angle, (4) beam-to-column flexural strength ratio, and (5) beam-to-column connection type/flexural stiffness and strength. The results of this parameter study are combined with the experimental results to select and improve the optimal design expressions for the unbalanced load. It is expected that this new design approach will improve the economy and seismic performance of chevron-configured SCBFs. A design change proposal based on this research has been submitted for consideration by AISC Task Committee on Seismic Design.

# Chapter 1 Introduction

## 1.1 Background

Architects and contractors prefer chevron braced frames for low- to mid-rise buildings for seismic design, because they accommodate architectural elements such as doors and windows, while providing the required lateral stiffness and resistance. This system was commonly used in older buildings, but chevron braced frames are not common in new construction, because current special concentrically braced frame (SCBF) design provisions require that the beam be designed to support the maximum expected unbalanced resistances of the tension and compression brace pair, considering severe compressive strength degradation). This assures that the plastic mechanism is brace buckling and yielding, and chevron braced frames meeting current code provisions require large and costly beams, and they are now much less common. Instead, for architecturally challenging configurations, engineers prefer different lateral-load resisting systems including buckling restrained braced frames (BRBFs) or reinforced concrete shear walls.

The history of concentrically braced frame design provides insight into the reasons for these changes. Prior to development of the AISC Seismic Provisions, the Uniform Building Code (UBC) controlled seismic design of steel structures. The 1982 UBC permitted the design of braced frames with few special design requirements including larger seismic design forces for braced frames, limited the grades of steel permitted in the braced frames and braced frame connections designs without the one-third stress increase permitted in allowable stress design (used for seismic design at that time).

Some of these requirements were tested as part of a large international program in late 1983 and early 1984, in which a full-scale six-story chevron braced frame was tested at the Building Research Institute in Tsukuba, Japan, as part of the US-Japan research program (Foutch et al. 1987, Roeder 1989, and Fukuta et al. 1989). Rectangular HSS braces with full-restrained (FR) connections to the beams and columns were employed. Most of the HSS braces would not meet the current SCBF local (b/t) slenderness limit, although a couple did come close. The chevron beams were not designed for the maximum unbalanced load required by current SCBF criteria and if measured properties for the braces and beams were employed, the demand-to-capacity ratios (DCR) for the current unbalance load requirement using expected design values were 2.6 and 1.9, for the bare beam and beam considering composite action respectively.

An unusual feature of the erection of this frame negatively impacted the system performance, since a variation of the Japanese Christmas tree erection procedure. Beam stubs of one half the beam length were welded to the column during fabrication, the columns were stood up, and the webs of the beam stubs were bolted together on erection. After erection, the flanges and webs of beam stubs were welded with CJP welds, and a relatively thick (5.5-inch concrete over 3-inch metal deck) composite slab was used. The bolted-welded beam splice occurred over the center of the chevron brace-to-beam connections. The frame was tested under small, moderate and large earthquake simulations. The small earthquake test was fairly linear and is not discussed. The moderate test (Miyagi-ken-Okii scaled to approx. 0.25g) resulted in some inelastic behavior with limited brace buckling. However, the nonlinearity was not understood until detailed inspection of the specimen after completion of the test. During this inspection, some permanent shear deformation was observed in the bolted-welded beam splices, which resulted from this short region acting as a short eccentrically braced frame (EBF) link. During the moderate earthquake test, one of these splices had pieces of steel torn out because the welds and bolts worked against one another. Because of this, all of these web splice zones were cut out and replaced by single, thicker welded plates for the large earthquake test.

The large earthquake test (Miyagi-ken-Okii scaled to approx. 0.5g) was then performed, and there was much more (mostly in-plane but some out-of-plane) brace buckling. The third-story brace had a large b/t ratio and sustained in-plane brace buckling; the brace fractured about two thirds of the way through the acceleration record. The test was stopped after brace fracture to save the overall frame for the moment-resisting frame (MRF) and EBF tests that followed. A number of influential engineers including Egor Popov, Vitelmo Bertero, Henry Degenkolb and Roy Johnston examined the frame shortly after this test. They noted and commented in some detail on the facts that 1) beams sustained permanent, downward deflection, 2) the slab was damaged, and 3) separation between the metal deck and the beam flange occurred. These observations lead to concerns about serviceability and repair issues rather than life safety or collapse issues.

Review of SEAOC Blue Book comments (Popov 1986, SEAOC 1990, and SEAOC 1996) suggest that these observations played a major role in revisions leading to current SCBF provisions for chevron braced frames. In the 1985 UBC, additional restrictions were added which focused on assuring that the beam can support gravity loads after brace buckling for chevron braced frame design. In the 1988 UBC, fairly significant revisions were added to braced frame design

requirements, and this specification was probably the first step toward the current SCBF requirements. Braces in chevron braced frames were required to be designed for 150% of the normal design load. In retrospect, the 150% design force was probably not a well-considered concept, because it could introduce other secondary problems such as increased column forces and connection issues. In the 1994 UBC, provisions fairly close to today's SCBF requirements were developed. The requirements for chevron braces eliminated the 150% strength requirement, but required that the beam be 1) continuous over the brace-to-beam connection, and 2) be designed for the unbalanced forces similar to what is in the current AISC *Seismic Design Provisions* (herein referred to as the *Seismic Provisions*).

## 1.2 Current Codes and Research

This brief historical perspective shows that the current design requirements for beams in chevron braced frames were greatly influenced by serviceability issues. As demonstrated above, practicing engineers and researchers were concerned about beam deflections and slab cracking more than life safety and collapse prevention; this is in stark contrast to the current seismic design provisions are focused on insuring low probability of collapse. Modern codes result in structures designed to sustain significant inelastic deformation during major earthquakes while limiting damage in small, frequent events, yet the *Seismic Provisions* have retained this serviceability concept during major seismic events for chevron braced frame design. Today the strength is magnified by  $R_y$  and a few other requirements, but the code provisions for chevron braced frames are founded on what was proposed in 1994. The current provisions have significantly reduced the use of SCBFs with chevron bracing. Chevrons are used quite often with BRBFs, but seldom used for concentrically braced frames.

Given this history, it is not clear that beam yielding in chevron braced frames adversely affects life safety and collapse prevention compared to other SCBF systems. An initial study of older braced frames began to study this issue. The study obtained design drawings for 12 braced frames designed for seismic demands in the 1960s, 1970s and 1980s (Sen et al. 2016b). All of these older buildings had some chevron bracing, and all of the chevron beams would fail to meet current SCBF requirements with beams strengths in the range of 12.5% to 20% of that currently required. This project also included experimental investigation of these older SCBFs. Of particular interest here are the results of a multi-story chevron braced frame with yielding beams by the current chevron beam strength requirement was tested at the NCREE Laboratory in Taiwan (Sen

et al. 2016a). However, the strength of the chevron beams one of several deficiencies relative to the *Seismic Provisions*. Figure 1-1a shows the force-drift behavior of this chevron brace with significant beam yielding. With composite action and a FR beam-column connection, the beam had 50% of currently required resistance, and the bare steel beam had 25 to 33% of currently required resistance. The beam-column connection was a welded shear plate connection. There were no shear connectors joining the beam to the slab, but there was limited composite action, since the metal deck was spot welded to the beam at intervals. Figure 1-1b was from a similar three-story test frame, and it had a strong beam that met SCBF beam strength criteria if composite behavior was considered. The beam had more than adequate shear connectors for full composite action, and the beam-column connections were welded-flange welded-web connections. The beam for the frame in Fig. 1-1b was 50% deeper and 110% heavier than that for the frame of Fig. 1-1a. The braces and columns were identical for the two frames and all members met AISC SCBF slenderness limits. The base shear was normalized by the same number for both frames.

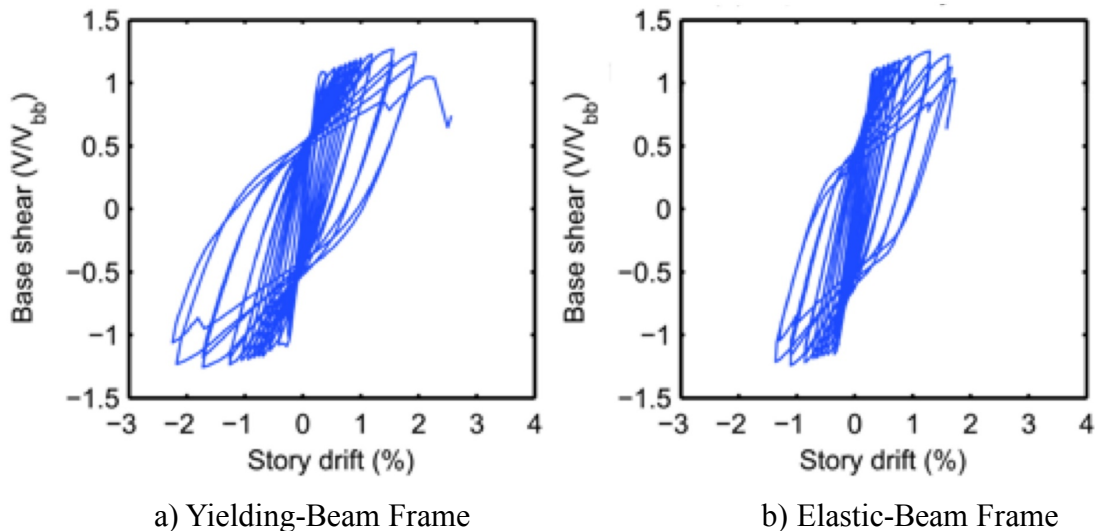


**Figure 1-1. Comparison of braced frame behavior: (a) chevron frame with a yielding beam, and (b) X-braced SCBF on the bottom two stories and a chevron with a strong beam on top story.**

Although the beam of Fig. 1-1a is much weaker, there is no difference in the resistance in the frame with the yielding beam. The story drift range (maximum drift in the positive direction + absolute value of the maximum drift in the negative direction) is approximately 4.5% for the yielding-beam frame. The frame has rectangular HSS braces, and so this figure suggests that any loss in deformation capacity is very modest. The frame in Fig. 1-1b had less deformation capacity, but the brace did not fracture. As with these older frames, there are other flaws, and an inadequate

weld with no demand critical weld requirements failed at another location. These two tests contradict the assumptions made in our design specifications and they call into question the justification of the required beam strength.

Other research supports these initial findings. Okazaki (2013) performed a shaking table tests of a single-story chevron on the Miki shaking table in Japan. This chevron braced frame beam was weak based upon its measured properties. If the bending resistance provided by the gusset plate is ignored the beam has 58% of current required resistance. If the beam-column connection develops plastic hinging in the beam, the beam has 71% of currently required resistance. The frame was subjected to three (3) earthquake levels of excitation and the force deflection behavior for each of the levels is shown in Fig. 1-2. As can be seen from the figure, brace buckling and the unbalanced force shows no deterioration of resistance. The rectangular HSS braces initially start to fracture at point 4 in Fig. 1-2c. At this point, the frame has sustained more than 3.5% drift range. This may be smaller than ordinarily expected, but the walls of the tube were relatively thin ( $D = 75$  mm, and  $t = 3.2$  mm. This has a slenderness equivalent to an HSS6x6x $1/4$ , which fails AISC slenderness limits.). This test also raises doubt about purportedly poor performance of chevron braced frames with yielding beams.

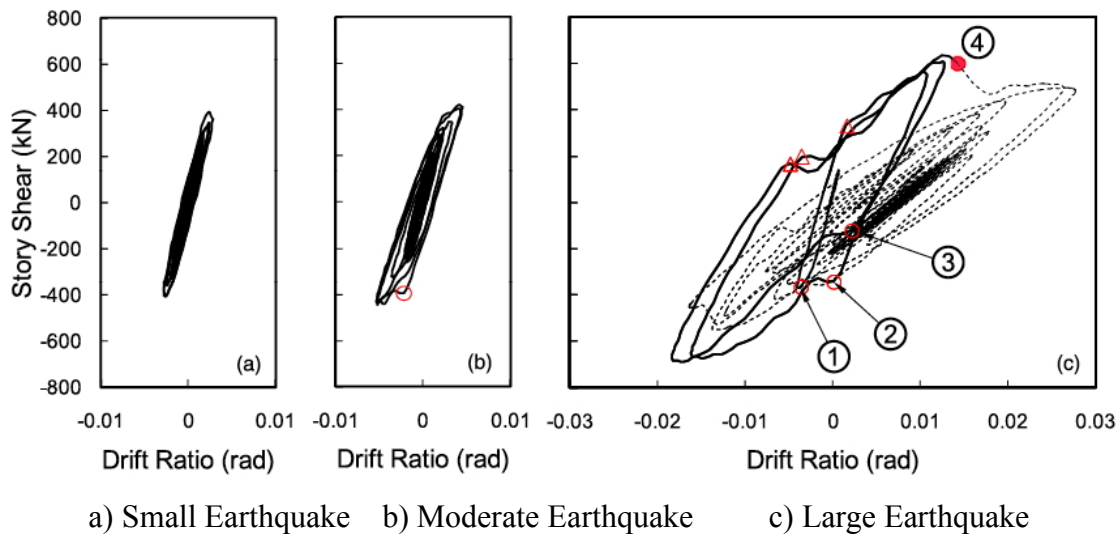


**Figure 1-2. Test results on a chevron frame with a yielding beam from Okazaki (2013)**

Nonlinear analyses of chevron braced frames were performed with both yielding and strong beams by AISC SCBF criteria, and the predictions are in strong agreement with these experimental observations. With yielding beams, the beam pulls down, but the maximum deflection during

extreme seismic events is not much more than 2 inches, unless the beam is extremely weak (i.e., less than 25 or 30% of current requirements). The braces sustain larger compressive deformation, but this does not weaken the frame. It is frequently argued that the important issue in brace behavior is not the story drift, but the drift range (Lehman and Roeder 2008). These tests and analysis are showing that the deformations of the brace are different for chevron-braced frames with yielding beams than for other braced-frame systems, but the range of deformation in the brace may be similar. The deformation of the brace is affected by the beam deflection, but there is a smaller effect on the drift range. The vertical deflection prevents the brace from fully yielding in tension. The brace will buckle and sustain compressive loading but the reduced cyclic strain demands drastically increases the fracture life of the brace, i.e. with the downward deflection of the beam, the tensile yielding of the brace is reduced and the tensile strain at the regions of local buckling are also reduced.

There are some research studies that appear contrary to these positive findings of chevron SCBFs with yielding beams. Tremblay and Robert (2001) performed nonlinear analysis using the DRAIN-2D computer program with a phenomenological brace buckling model developed from the US-Japan program. The braces were modeled with pinned end connections, and all beam-column connections and column splices were also modeled as pinned connections. The chevron beams were designed to develop 60%, 80% or 100% of the nominal chevron brace yield load. The results of these analyses suggest that limited chevron beam yielding may be tolerated with shorter buildings, but taller buildings suggest a tendency for deterioration of performance, concentration of damage into a single story, and potential collapse or stability failure. However, more advanced modeling found contrary results, with more realistic brace buckling and fracture model and inclusion of rotational and axial springs to model the gusset plate and beam-to-column connections.

A more recent study (Balazadeh-Minouei et al. 2018) on the seismic performance of existing chevron braced frames with ASCE 41-13 linear dynamic and nonlinear dynamic procedures was performed with the OpenSees computer program. Beam-column connections were again modeled as pinned. While there are clear limitations in the ASCE 41 procedures for evaluating braced frames, the general conclusions of this study were similar in that significant seismic upgrade was typically required. Again, these models have limitations because of the assumptions made about the connections.

### **1.3 A Comprehensive Research Study**

The work described above lead to initiation of a comprehensive research study funded by the American Institute of Steel Construction (AISC) to investigate the effects of chevron beam yielding on the seismic performance of chevron braced frames. The work was divided into 3 phases. Phase 1 included testing and analysis of single-story chevron braced frames to evaluate the effect of various levels of beam resistance of braced frame performance. This work established basic performance of chevron-braced frames and initial recommendations. Phase II consisted of testing of a 3-story chevron braced frame and analysis of multi-story braced frames to evaluate multi-story effects and further refine the design procedure. The results of Phases I and II are the basis of the research described in this report and are summarized in Chapter 2.

The experimental research was generally performed at the University of Washington (UW), but the 3-story braced frame test of Phase II was tested at the National Center for research in Earthquake Engineering (NCREE) laboratory with Taiwanese and UW researchers with aid and guidance of Prof. K-C Tsai. The first two phases clearly show the potential benefit from chevron braced frames with beam yielding and plausible design strategy for this beam yielding. Using these results as its foundation, Phase III of this research is a nonlinear analytical study to evaluate the effect of the proposed provisions on a wider range of chevron braced frames that may be encountered in design. Chapter 3 describes the analytical models and the range of parameters considered in the study. Chapter 4 describes the general results of the analysis, and includes a limited study of the dynamic time history of chevron braced frames with yielding beams and other braced frame systems. Chapter 5 evaluates these results in greater detail to drawer broader conclusions from the work. Chapter 6 summarizes the results and conclusions.

## Chapter 2 – Summary of Phase I and II Research

### 2.1 Summary of Phase I

Six large-scale single-story chevron braced frames were tested at the UW under cyclic loading to large drift demands. The first four tests (Chevrons 1-4) were chevron braced frames with identical columns, braces, connections and frame geometry, but different beams sections to evaluate the effect of beam strength (i.e., beam yielding) on frame performance. The braces were all A1085 HSS4x4x<sup>5</sup>/<sub>16</sub> braces.

The reference specimen, Chevron 1, was designed to meet the current AISC SCBF requirements for the prescribed unbalanced vertical and horizontal loads, which assume full expected tensile force of the tension brace and degraded expected compressive force in the compression brace (degraded to  $0.3P_{cr}$ ). Chevrons 2-4 were designed with beams that had approximately  $\frac{1}{2}$ ,  $\frac{1}{3}$ , and  $\frac{1}{4}$  the current AISC required strength; these strengths were quantified by comparing the demand of idealized unbalanced vertical load to the plastic capacity of the one-story system assuming beam yielding on either side of the gusset plate. This actual strength ratios were 114%, 55.5%, 35.3% and 23.1% for these for specimens. Two additional specimens (Chevrons 5 and 6) investigated the impact of brace type and beam stiffness. Chevron 5 used ASTM 500 HSS4x4x<sup>5</sup>/<sub>16</sub> braces and W 14x31 beam (beam strength comparable to Chevron3). The results of Chevron 1- 4 indicated a possible increase in ductility to brace fracture for the ASTM 1085 braces; since ASTM 500 Grade C HSS braces are more common and were used in prior test programs. To retain the specimen geometry and limit changes in the setup, the first five specimens all had W14 beams, but Chevron 6 used a deeper beam section (W21) which has greater stiffness and approximately the same flexural resistance as the beam used for Chevron 2 (W14) section. This change caused some changes in frame geometry, but it evaluated the effect of beam stiffness in combination with beam yield behavior.

All six specimens were tested under a cyclic inelastic deformation protocol with increasing drift levels. Strains, deflections, loads and deformations were continuously monitored during the entire test to fracture of both braces and limited large inelastic cycles were continued for several cycles after both braces fractured. The data was analyzed and interpreted with particular attention paid to the lateral resistance, story drift, moments and shears of the beams and columns, axial load and deformation of the braces, and the beam deflections. The results indicated that: (1) an decrease

in beam resistance results in increased frame drift capacity prior to brace fracture and beam deflection; and (2) the base shear capacity and tensile demand in braces decreased with increased beam yielding (ie decreased beam strength) but this decrease is not a linear relationship and (3) beam resistance greater than about 33% of the current requirements resulted in nearly the same shear strength and tensile-brace demands as provided by current SCBF designs. The tests also demonstrated the increased ductility resulting from using ASTM 1085 grade HSS section braces. Comparison of Chevrons 2 and 6 showed that the only real difference in behavior for deep and shallow beams with the same iDCR values is that the deeper beam has smaller elastic deflection due to its larger moment of inertia.

The second part of the Phase I research used experimentally-validated, high-resolution finite element modeling to conduct a parametric study to evaluate untested values of beam strength and stiffness. High-resolution nonlinear computer models were developed for each of the test frames using the ABAQUS nonlinear finite element program. These analyses simulated the cyclic frame deformations up to brace fracture for all tests. The local and global observed response, including yielding and buckling, and measurements, including story drift, brace out-of-plane deflections, and beam deflections, of each test were compared to the numerically simulated behavior to validate the modeling approach.

The resulting computer models were then evaluated other design parameters including d beam strength, beam depth and different connection types. The simulated and measured results demonstrate a change in slope in the behavior at beam strengths in the range of 25% to 33% of current requirements. Further, the maximum lateral resistance is larger than the nominal beam resistance less than about 33% of current requirements. This comparison suggests that the minimum beam strength that would be practical for design would be in the range of 33% to 40% of current requirements, since beams which are stronger than this limit are expected to develop their full design lateral resistance and deformation capacity.

## **2.2 Summary of Phase II**

For Phase II, a 3-story chevron braced frame with beam yielding and a beam with approximately 40% of currently required resistance based upon a restrained beam plastic collapse mechanism was tested at the NCREE laboratory in Taiwan. The specimen was designed to be at or near the limits of desirable performance from the single-story test results. The beam column connections were welded-flange-welded-web connections. The frame was loaded at the top slab

to provide constant story shear over the height of the structure. The bottom two stories of this frame evaluated the yielding beam chevron behavior, since the top story was conservatively designed to assure that lateral loads could enter the frame through the top story slab. Extensive instrumentation including strain gauges, LVDTs, potentiometers, tilt meters, and Optitrak deformation measurements were included. The 3-story specimen provided very good inelastic behavior, but the test was ended due to a column flange fracture rather than the usual brace fracture. This column fracture was caused by the concentrated stress and strain due to the relatively rigid top story. The 3-story frame had had relatively axial loads in the bottom story beams, because the large reduction in beam size increased the effect of axial loads which are not reduced by beam yielding. The combination beam twist, the corresponding increase in effective length and reduction in buckling resistance with increasing story drift combined with the large axial load in the bottom level beams resulted in slightly greater deterioration of lateral resistance than anticipated. Experimentally-validated nonlinear analyses again were performed with ABAQUS extend the results of the experiment and to evaluate proposed design methods.

Nonlinear computer models of 3-story and 9-story braced frames were developed in Phase II using the OpenSees computer program. First, the modeling approach was updated and validated using the experimental force-displacement test results. A fracture model was developed to simulate brace fracture for the chevron configuration. The results of the tests indicate that the fracture life of chevron-braced frames is extended, and the validated modeling approach, including the new fracture model, was used to conduct nonlinear time history analyses, which showed that chevron CBFs with yielding beams will provide inelastic performance that is comparable or better than that achieved with other SCBF systems if the beam resistance is controlled.

All of the building models were subjected to 30 two-component earthquake-acceleration records at three hazard levels: 10% in 50-year recurrence interval, 2% in 50-year recurrence interval and 1% in 50-year recurrence interval. The story drift, beam deflection and brace fracture for all story drifts were evaluated. Statistical variation in performance for the different frame designs at the various performance levels were evaluated. The seismic performance of chevrons with yielding beams were found to meet the design intent providing low probability of collapse in the 2% in 50-year hazard.

### **2.3 Observations and Conclusions**

A number of observations and conclusions were drawn from this research.

- The inelastic story drift achieved prior to brace fracture was larger for chevron-braced frames with beam yielding than for chevron braced frames designed by AISC SCBF criteria. The drift capacity was larger with increased beam yielding.
- Chevron-braced frames with yielding beams achieved larger story drift prior to brace fracture than other braced frame configurations with the same braces and geometries. This occurs because yielding beams result in increased downward beam deflections, which increase compressive deformations and reduce the maximum tensile strain demands of the brace. Brace fracture is primarily driven by tensile strains in the locally damaged area caused by brace buckling, fracture is delayed.
- The lateral resistance of the frame decreases slightly with beam yielding, but the decrease is smaller than the reduction in beam resistance. The lateral resistance remains stable without significant deterioration and is consistently larger than the resistance required from a linear-elastic analysis using the design loads if the beam has more than 40% of current SCBF unbalanced load. The axial load in the beam becomes increasingly important in the beam design, when reduced unbalanced forces are used.
- As expected, vertical deflections of the beam increase with decreased beam strength, but the deflections were consistently smaller than would be expected given the reduction in beam resistance. Residual deflections after lateral load was removed were typically less than 2 inches or  $1/120$  of the span length if the beam was strong enough to develop more than  $1/3$  of the current strength requirements.
- Braces buckle in compression for all yielding beams. The experimental and simulated results indicate that the degradation in compressive brace force is negligible if the beam resists more than 33% of current AISC SCBF unbalanced load, and the maximum axial load in beam due to the elastic brace forces is less than 50% of the tensile yield of the beam. With beam yielding, the tensile brace force is much less than yield and decreases with increased beam yielding. The maximum tensile force of the brace decreases with decreasing beam resistance.
- There are two cases of maximum brace forces that must be considered in design of yielding beams. Both cases result in combined loading from the axial and flexural demands. The first is associated with both the tensile and compressive brace acting at their maximum elastic resistance. For the second, the beam must resist the bending moment associated with the unbalanced load when the brace has its maximum tension force and its deteriorated

compressive force. With the current unbalanced load requirements, the second criterion automatically controls and the first criterion is met automatically. For yielding beam chevron systems, the second criterion results in a lower unbalanced force than chevrons with non-yielding beams, but the first criterion is largely unchanged. Therefore, the first criteria may become significantly more important with adoption of these changes.

- Analyses of the X-braced frame and Chevron braced frame show that the probability of brace fracture and frame collapse are decreased for chevron braced frames when compared with buildings with multi-story X-brace configuration.
- Although it has been suggested that chevron-configured SCBFs concentrate nonlinear demands to a single story, these results demonstrate that chevron bracing does not have any greater tendency to concentrate inelastic deformation than other brace configurations. Prior analytical research may have overestimated this concentrated damage effect with yielding chevron beams by using pin connections to join the beam and the brace to the column. Analysis shows greater tendency for deterioration of resistance and concentration of damage as the connection restraint is reduced, but gusset plate connections are not pinned connections.

### 2.3 Recommendations

It is recommended that yielding chevron beams be permitted for seismic design, and the following design procedure is proposed.

1. Design the braces be designed to develop the total story shear required by ASCE 7
2. Determine the expected tensile force ( $P_{ye} = A_g R_y F_y$ ) and expected compressive force ( $P_{cre} = A_g R_y 0.658 \frac{R_y F_y}{F_E} F_y$ ) of the braces.
3. Design the beam for Load Case 1 where the tensile brace develops  $P_{ye}$  and the compressive brace develops  $P_{cre}$ .
4. Design beam for an unbalanced load due to Load Case 2 where the compressive brace develops a force of  $0.3P_{cre}$  and axial load in tension of magnitude  $P_{cre}$ .
5. Proceed normally with capacity design of the columns and connections for the  $P_{ye}$  and  $P_{cre}$ .
6. The remainder of design using the conventional design process.

## Chapter 3 – Overview of Modeling Approach and Parametric Study

The experimental and analytical work of Phases I and II showed considerable potential for chevron braced frames with yielding beams. The work demonstrated that chevron-braced frames with yielding beams developed their design lateral resistance and retained this resistance through large inelastic deformation. Further, the braced frames were able to develop larger inelastic deformations prior to brace fracture than chevron braced frames designed by current AISC SCBF criteria. However, it was noted that the prior study focused on specific braced frame geometries with a narrow range of brace sizes and slenderness ratios. As a result, Phase III of this research was a parameter study was initiated to broaden the results of this research to the full range of possibilities of design for building structures.

### 3.1 Goals and Scope of Parameter Study

The nonlinear analytical parameter study was performed with the OpenSees computer program. The models were verified and documented by comparison with the experimental results. The parameters were varied so that the full range of parameters that engineers may encounter in design were investigated. The goals of the analysis were to verify that (1) chevrons with yielding beams designed by proposed procedure develop and retain their design resistance; (2) chevrons with yielding beams designed by proposed procedure do not cause early brace fracture or other detrimental behavior; (3) chevrons with yielding beams designed by proposed procedure do not exhibit greater deterioration of resistance or concentration of deformation into single stories than other SCBF systems. The following parameters were investigated:

1. Beam tension-to-compression ratio. To date only two brace sizes have been tested. Depending upon the global slenderness ( $Kl/r$ ) of the brace and the beam design, the tension-to-compression ratio of the brace could vary widely.
2. Brace angle. These experiments and analyses have been performed with braces near 45 degrees. This is likely a fairly common angle for chevron bracing, but braced frames commonly have bracing with angles of inclination between 30 and 60 degrees.
3. Beam to column flexural strength ratio. In the 3-story test, the column was designed to develop the full expected tensile and compressive capacity of the braces. However, with yielding beams in chevron braced frames the brace never develops anything close to its expected tensile

force. The maximum tensile force in these systems is approximately the same as the magnitude of  $P_{cr}$ . Recognition of this in the column design requirements could result in significant cost savings for chevron braced frames.

4. Beam flexural strength and stiffness in multi-story frames. Single-story Chevrons 3 and 6 investigated the influence of beam stiffness on chevron braced frames. The results indicated that there was little difference in the behavior, since the difference appeared to be totally related to the reduced elastic deflection of the chevron beam with larger moment of inertia. A limited analytical study including consideration of the dynamic time-history response may be beneficial.

### **3.2 Construction and Verification of the Computer Model**

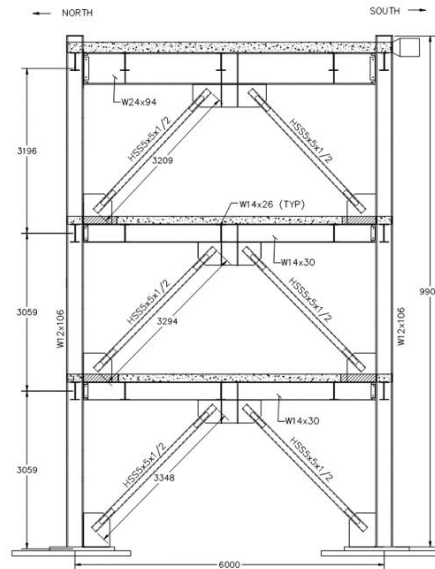
The 3-story chevron frame with yielding beams tested at the NCREE laboratory in Taiwan serves as the basis of analytical model used for Phase III of the research study. This frame is illustrated in Fig. 3-1. As part of Phase II, this frame was analyzed with a high resolution nonlinear finite element analysis with the ABAQUS computer program. With this prior analysis, the steel frame was modeled as tested in the test apparatus with a fine mesh of shell elements, and the composite slabs were model as 3-dimensional solid elements as shown in Fig. 3-2. The analytical results were compared to the measured experimental behavior as shown in Fig. 3-3 (Roeder et al. 2019). The loads were applied through the slab of the top level, and hence the top floor had a heavier beam, thicker slab, and more shear connectors than would be expected in practice to accommodate the load transfer required by the test setup.

Figure 3-3 shows that the model is capable of simulating the full nonlinear (material and geometric) response of the system. Good comparison was also achieved with local behaviors including local buckling, plastic hinging, out-of-plane deformation of the brace and vertical beam deflection. Both models accurately predicted the inelastic deformation of the second story and both models underestimated the inelastic deformation in the bottom story. The model with the composite slab more accurately estimated the frame resistance at smaller story drift, but the bare steel more accurately simulated the behavior at larger inelastic deformations. During the experiment, separation between the concrete slab and steel beam was noted. This indicates that composite action is lost during the larger deformations expected during severe earthquakes. The two models bound the response. Hence, the bare steel model was selected as the more reliable indicator of the response prediction for chevron braced frames with yielding beams. It is a more

reliable predictor of the inelastic deformations expected during severe earthquakes, and it is a bit conservative in the prediction of maximum and sustained resistance. This bare steel model was used as the basis of an initial parameter study on chevron-beam yielding with the ABAQUS computer program, and it was used as the basis of the analysis of verifying the OpenSees analysis performed in Phase III of this research.



Photograph of Test Frame and Setup  
(Note: blue members comprise the out-of-plane restraint frame and not the specimen)



Elevation Drawing of Test Frame  
(all units in mm)

Figure 3-1. Three-Story Test Frame

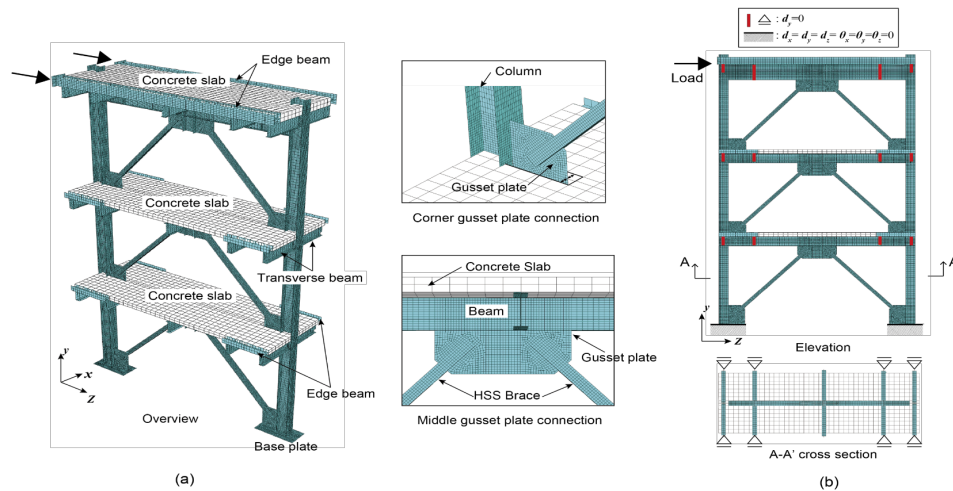
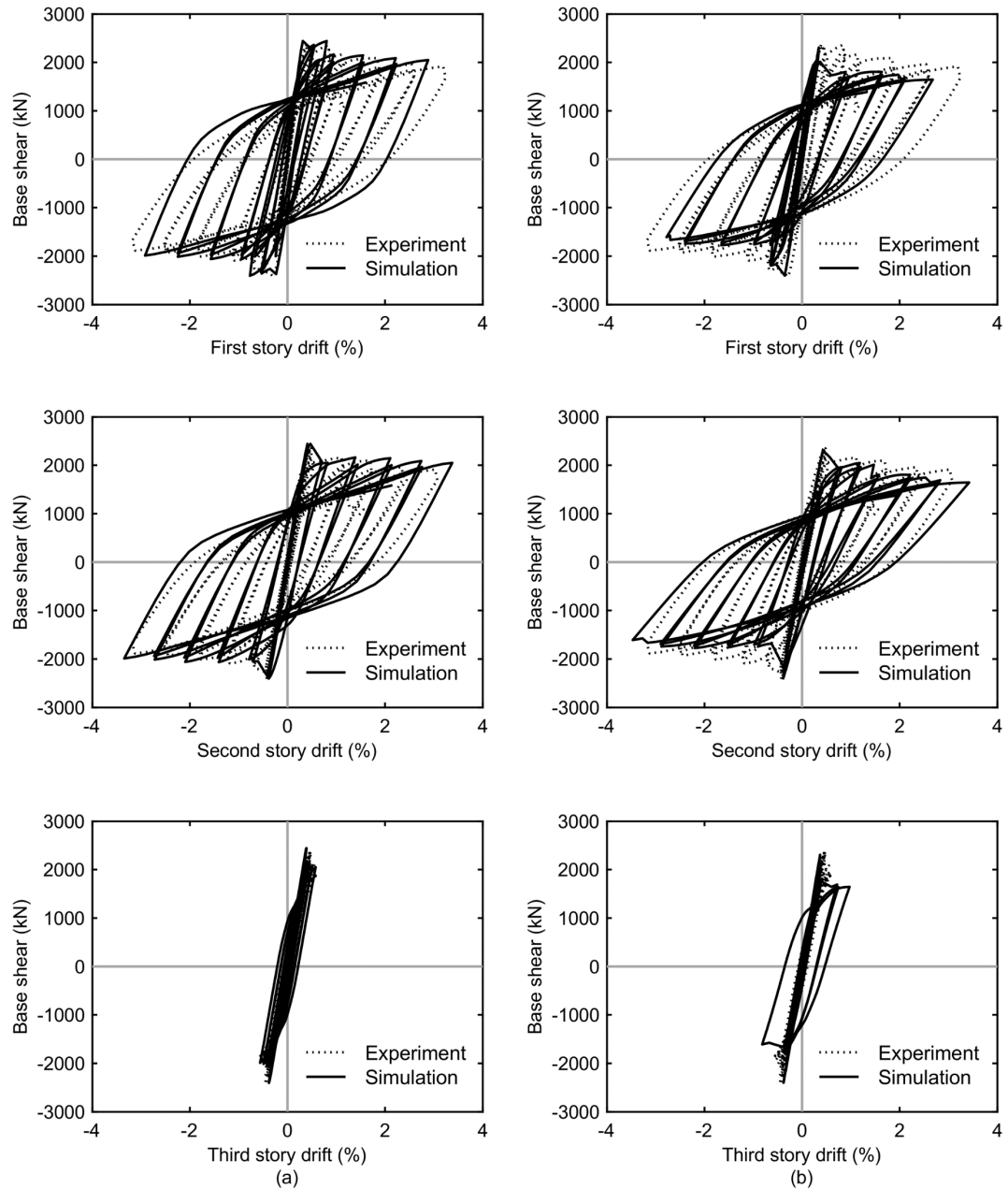


Figure 3-2. Analytical Model: (a) Finite Element Mesh and (b) Loading and Boundary



**Figure 3-3. Computed Results: (a) Model with slab and (b) Model without slab**

While the ABAQUS computer program provides good estimates of local and global behavior during severe inelastic deformation, it is impractical for use in this Phase III research. Phase III analysis requires a much larger number of analytical models, and ABAQUS is extremely costly in the development of the models and in computer time for executing the analyses. Hence, the OpenSees computer program was selected for this phase of the research.

The OpenSees model will not simulate some local behaviors such as local cupping of the brace, but it can accurately simulate development of brace buckling, plastic hinging, out-of-plane deformation of the braces, vertical deflection of the beam, and global resistance and deformation of the frame. In addition, the research team has developed models to accurately simulate brace fracture and nonlinear behavior after brace fracture. The ATC-114 program has proposed techniques for accurately simulating the inelastic behavior of concentrically braced frames, and these techniques and other methods developed in recent research were used to simulate the braced frames in this phase of the research as follows:

- Members were divided into fibers as illustrated in Fig 3-4.
- Each brace was modeled using displacement-based fiber-cross section beam-column elements divided into 16 segments with five integration points per element. and an initial displaced secant shape approximating a sine function with out-of-plane amplitude of  $L/500$ , where  $L$  is the clear brace length.
- The steel beams and columns were modeled using force-based beam column fiber elements using OpenSEES Steel02 material model with five integration points. Cyclic deterioration of the beams and columns was not considered because: (i) the sections meet the highly ductile compactness requirements of the Seismic Provisions, (ii) the rotation demand on the beams is small, and (iii) comparison of the performance between the various frames depends largely on the differences in brace demand and behavior.

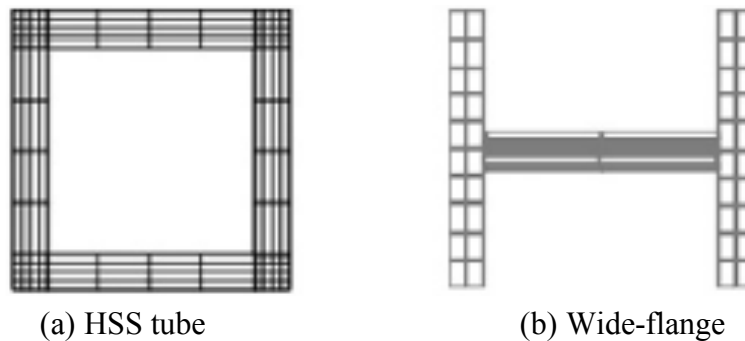


**Figure 3-4. Schematic layout of fibers for HSS and wide flange cross sections.**

- Connection modeling extensively used nonlinear springs. Gusset plate connections have significant impact on braced frame performance, and in particular, corner gussets provide increase connection stiffness causing plastic hinge formation in the beam near the corner gusset. As a result, gusset plates were modeled with a series of rigid links and nonlinear

springs as shown in Fig. 3-5. The gusset plate was modeled as a nonlinear rotational spring as shown in Fig. 3-5. The flexural resistance of the spring depends on the gusset plate thickness, yield strength, and the Whitmore width; the post-yield stiffness was taken as 10% of the initial stiffness. The spring requires calculation of an effective length of the gusset plate, as follows:

$$L_{ave} = \frac{1}{3}(L_1 + L_2 + L_3) \quad (\text{Eq. 3.1})$$

where  $L_1$  and  $L_3$  are the lengths from the end of the Whitmore width to the intersection with the column and beam flanges, respectively, and  $L_2$  is the distance from the end of the brace to the beam or column flange, as shown in the figure.

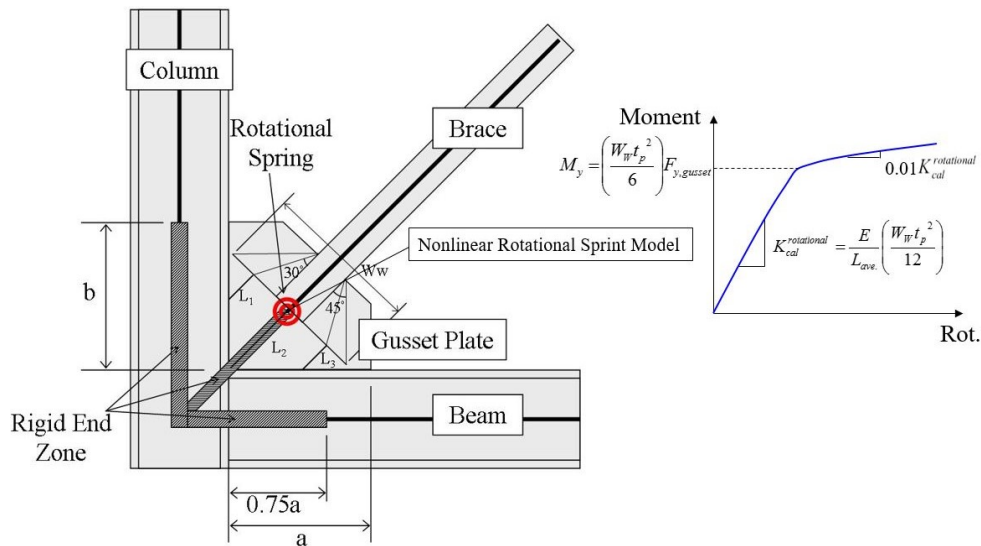


**Figure 3-5. Rotational connection model of corner connections (Hsiao et al., 2012).**

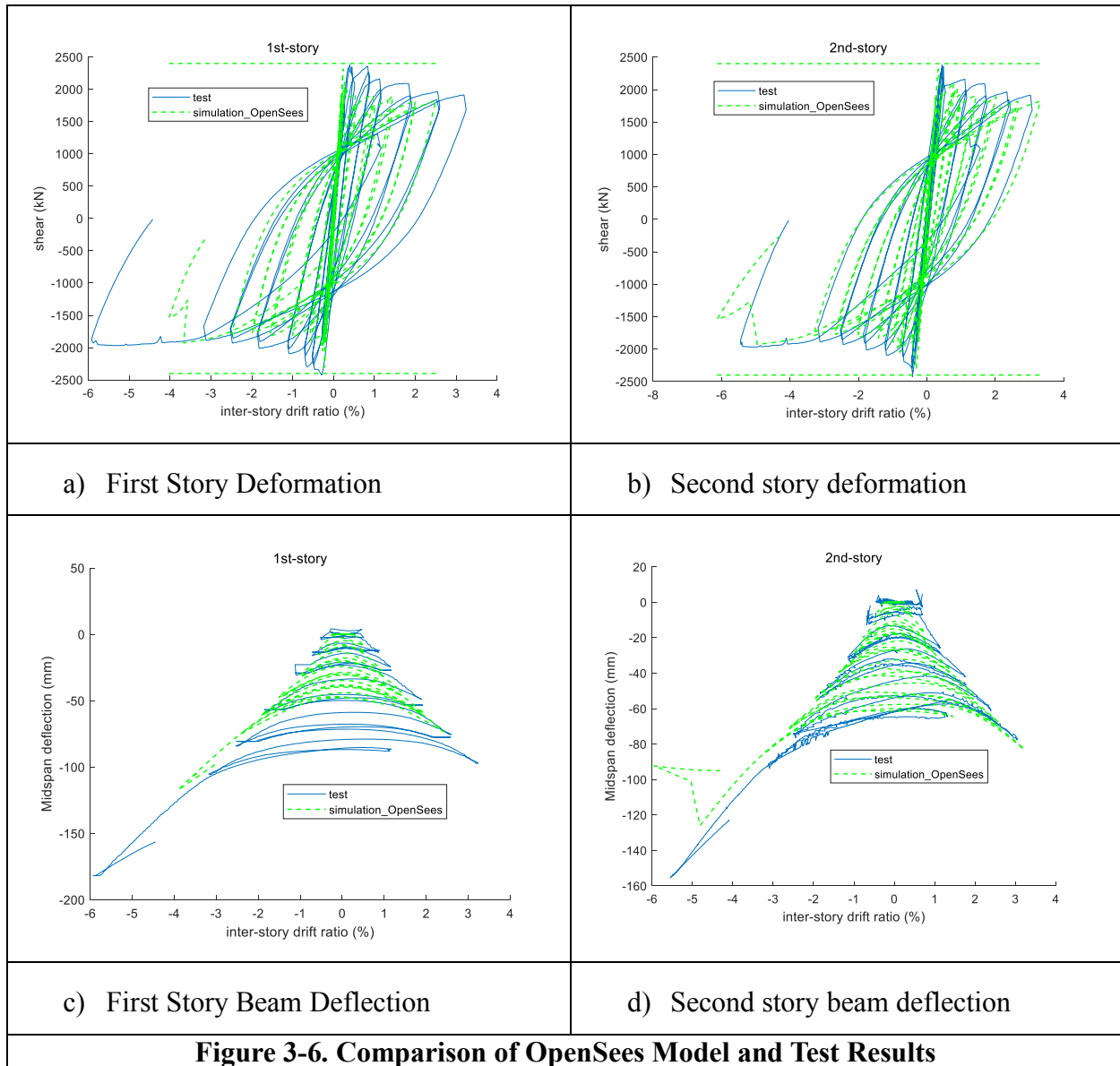
- A fracture model was utilized to simulate brace fracture. The model simulates fracture by reducing the strength of the fractured fibers of brace cross section using a Maximum Strain Range (MSR) material (Hsiao et al. 2013), where the MSR is maximum difference between the minimum and maximum strains throughout the deformation history. Strength of the fiber is lost once this value exceeds the MSR limit,  $MSR_{f,disp}$ , as given in Eq. 3.2. The original model by Hsiao was updated by Sen (Sen et al. 2019) to account for the asymmetry in the demand for braces in chevron configurations which elongates the fracture life of the brace as observed in recent tests (Roeder et al. 2017, Ibarra 2018).

$$MSR_{f,disp} = 0.554 \left( \frac{b}{t} \right)^{-0.75} \cdot \left( \frac{KL_c}{r} \right)^{-0.47} \cdot \left( \frac{E}{F_y} \right)^{0.21} \cdot \left( \frac{\delta_{c\_max}}{\delta_{t\_max}} \right)^{0.008} \quad (11)$$

In the expression  $b/t$  is the local slenderness ratio;  $KL_c/r$  is the global slenderness ratio, in which  $r$  is the moment of radius of gyration with respect to the buckling axis;  $E/R_y F_y$  is the ratio between the Young's modulus and the expected yield stress of the brace; and  $\delta_{c\_max}/\delta_{t\_max}$  is the ratio between axial compressive and tensile deformation of the brace. A single fiber fractures once its MSR reaches  $MSR_{f,disp}$  then full brace fracture, and element removal to prevent numerical convergence issues, is triggered once 50% of the fibers fracture. It is of note that the test data used for the calibration had few results for very large cross-section braces, and the model accuracy may be limited for these sections.

- The OpenSees model did not include the benefits of the composite slab, however prior discussion of the ABAQUS modeling shows the rationale for and benefits of neglecting composite action.

This modeling approach was used to model the braced frame from the recent Taiwan test (see Fig. 3-1). The results of comparison of the computed results from the OpenSees model to the three-story test results are shown in Fig. 3-6. The figure shows that the OpenSees models compares to the experimental results similarly to comparison of the bare steel nonlinear ABAQUS analysis to the experimental results. The bare steel OpenSees model underestimates the maximum resistance, because the composite behavior is neglected. Therefore, this model will be a conservative estimate of resistance. The second story deformation is accurately predicted, but the top story was overestimated (not shown in figure) and bottom story was underestimated in the computer model. The top story of the test frame had a very stiff, strong beam and slab because of the loading apparatus used in the test setup. This added top story stiffness is not fully simulated in the bare steel models, because much of the test frame top level strength and stiffness is provided by composite action, and so the top story experiences limited inelastic deformation and the inelastic demands on the bottom story are subsequently reduced in the bare steel computer models. The modeling procedure closely simulates the global and most local results of the ABAQUS model, and compares conservatively but reasonably well to the test results. Therefore, this modeling approach was used for this Phase III parameter study.



### 3.3 Adaptation of the Computer Model to Parameter Study

Although the model was validated using the 3-story test, this was not the right configuration for the basis of the study since a number of aspects of that model were used to meet the requirements of the test apparatus and are not reflective of design practice. As such, the frame for the parameter study was redesigned. The redesigned frame had the same frame geometry and brace sizes for all story levels, and the loading remained still a constant top story, cyclic shear loading. (This is analogous to a braced frame with the mass only at the top story). The displacement-controlled loading used in the test and prior analysis were retained and used for all analyses.

The primary difference are as follows:

- The test frame had W14x30 beams for the bottom two stories, and this beam is under-designed by the proposed design criteria provided in Chapter 2. Using the design criteria, the beams used for the bottom two stories of the test frame were W14x48.
- The top beam (W24x94) was extremely strong to accommodate the loading apparatus, and this beam was clearly overdesigned by the proposed design criteria. The top beam was now designed to the proposed criteria. The beam for the top story is a W14x61. The top story still has a slightly larger beam, because the top story has no corner gusset plate, and this leads to a longer effective span length and larger moment resistance required to resist the unbalanced load.

Figure 3-7 shows the computed behavior for the frame when subjected to the roof deformation-based load protocol used for the Taiwan test. With this redesigned frame, the story drift is well distributed over the frame height. The 2<sup>nd</sup> and 3<sup>rd</sup> stories sustained somewhat larger inelastic deformations than the first story, but all stories had significant inelastic deformation.

The dashed and dotted horizontal lines indicate the design and expected capacities of the frame solely resulting from the two braces achieving the compressive capacity of the braces in both tension and compression. It can be seen that the full expected compressive force of the brace,  $P_{cre}$ , was developed in both directions and the maximum tensile force in the braces had the same magnitude as  $P_{cre}$ . The nominal design resistance of the frame,  $2\cos\theta P_{cm}$ , based on the nominal yield stress is retained to the 3% story drift (6% drift range). It can be seen that even at 3% story drift, the maximum beam deflection is no more than 3 inches. Which is less than 1/80<sup>th</sup> of the span length. Figures 3-7e and f show the force-deflection response of the 3<sup>rd</sup> story braces. The braces all achieved the expected buckling resistance,  $P_{cre}$ , in compression, and the magnitude of the tensile force in the brace did not exceed the magnitude of  $P_{cre}$  as postulated in the proposed design method. Based on the analyses, none of the braces were expected to fracture, and the analysis with the revised top story beam design showed no indicated of column fracture, as noted in the test specimen, as expected.

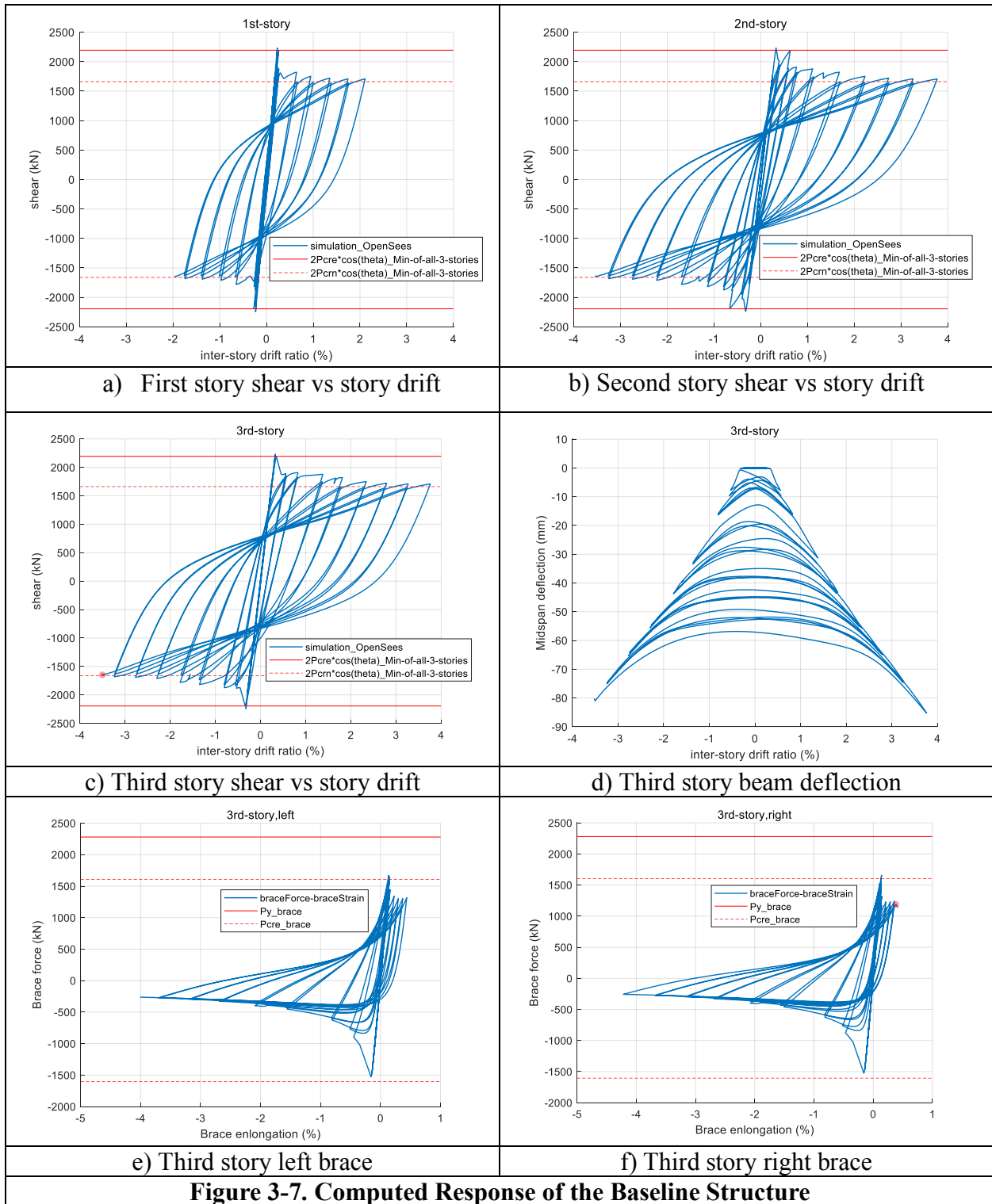


**Figure 3-7. Computed Response of the Baseline Structure**

This reference frame is the base line analysis for the remaining parametric study. The analytical method will be applied to other brace sizes and frame geometries to evaluate the effect of the design proposal with different design parameters. In each case, a beam design was

conducted using the proposed (yielding beam) and current SCBF procedures for chevron braced frames. The analysis showed that real benefit of the proposed procedure occurs with more slender braces where there is considerable difference between  $P_{cre}$  and the expected tensile yield force,  $P_{ve}$ .

A third alternative, which is not a primary focus of this report was also considered. In this third design approach,  $P_{cre}$  is calculated without the amplification of 1.14 on the theoretical buckling load. This 1.14 factor is appropriate for slender braces, because of past research showing that columns with elastic buckling sometimes buckle at loads slightly smaller than the Euler buckling load due to initial crookedness and imperfections of the column. A design factor 0.85 or 0.877 has historically been applied to the Euler resistance for steel design, and the 1.14 is the inverse of this factor. However, the seismic provisions apply the 1.14 to all braces regardless of slenderness. It could rationally be argued that this 1.14 factor need not be applied for braces where:

$$\frac{L_c}{r} \leq 4.71 \sqrt{\frac{E}{R_y F_y}} \quad (\text{Ea. 3.3})$$

It should be noted that different column sizes were required for different brace sizes and different frame geometries. Columns were always sized to meet the current brace forces for all three design methods. All analyses were performed on 3 story frames, and all additional analyses will continue until brace fracture occurs, since this is the likely initial failure mode for concentrically braced frames. The deformation protocol was necessarily increased beyond the test protocol for some cases.

### 3.4 Scope of Analyses

Seven frames were designed and analyzed to accomplish the model development and verification described earlier. Thirty-seven different combinations of frame geometry and brace size were evaluated as part of the parameter study. Using the three variations for design, 111 chevron beam combinations were designed and analyzed for nonlinear behavior. The broader goals of these analyses were to determine if the proposed design method resulted in unacceptable behavior under some design conditions. The behavior of the frames was analyzed to:

- Establish whether chevron-braced frames with yielding beams designed by the proposed method behave equal to or better than chevron-braced frames design by current criteria.
- Determine whether chevron-braced frames with yielding beams designed by the proposed method develop some premature failure criteria such as brace fracture.

- Establish whether chevron-braced frames with yielding beams designed by the proposed method develop the expected lateral resistance and retain their nominal design resistance through significant inelastic deformation.

There is considerable interaction between the parameters in the study and therefore it is not possible to investigate them independently. For example, brace slenderness,  $Kl/r$ , is clearly affected by brace size, but it is also affected by frame geometry. To evaluate the global goals, seven brace sizes were analyzed (HSS3x3x<sup>3</sup>/<sub>8</sub>, HSS4x4x<sup>1</sup>/<sub>2</sub>, HSS5x5x<sup>1</sup>/<sub>2</sub>, HSS6x6x<sup>1</sup>/<sub>2</sub>, HSS7x7x<sup>1</sup>/<sub>2</sub>, HSS7x7x<sup>5</sup>/<sub>8</sub>, and HSS10x10x<sup>5</sup>/<sub>8</sub>). These brace sizes run from very compact to slightly outside the AISC Seismic Provision requirements for *highly ductile elements* which are required for SCBFs. The column spacing story height of the baseline frame were 6000mm (19.7 ft) and 3059mm (20.0 3 ft). These dimensions were the same as those used for the three-story test described above. However, column spacings of 4500 mm (14.75 ft) and 9000 mm (29.5 ft) were also analyzed. The combination of 7 brace size story heights 3000 mm (9.8 ft), 4500 mm (14.75 ft) were analyzed. The combination of 7 brace sizes, 3 column spacings, and 2 story heights lead to 42 possible combinations, and 37 of those combinations were evaluated for the 3 different design cases, i.e., the current AISC requirements, the proposed requirements, and the proposed requirements without the 1.14 factor in computing  $P_{cre}$ , to complete the variation of parameters for this study.

## Chapter 4 – Analytical Results

### 4.1 Parameter Study Analysis

The results from the 111 nonlinear parameter analyses are summarized in this chapter. Using the test loading protocol, the deformations were increased until brace fracture was estimated by the computer model. Table 4-1 summarizes each frame that was analyzed, including sections used, geometry, and material strengths as well as the global results. It is of note that only the member sizes of the columns, braces and beams for the lower two levels are presented since these are the stories that sustained inelastic action. The top beam was slightly larger than the lower stories, but its size is not given in the table.

The drift range corresponding to brace fracture is provided in the table (note that for analyses that predicted a drift range greater than 16%, the value is indicate as >16% since it is postulated that the connections cannot sustain story drifts larger than 8% in each direction). For a given brace size and frame geometry, the brace with beam designed by the proposed achieved the approximate deformation or a significantly larger deformation than that achieved by the braces with beams designed by the current SCBF criteria. This is consistent with the experiments and analysis of the Phase I and II research. A brief examination of the data shows that the proposed method had significantly lighter beams and achieved significantly larger deformations prior to brace fracture with larger  $Kl/r$  values than did braces with beams designed by the current SCBF criteria. Braced frames with low  $Kl/r$  values resulted in nearly identical behavior for beams designed by all three methods.

**Table 4-1. Summary of Parameter Analysis Results.**

ID	Brace Cross-section (Material Spec.)	Column (A992)	Beam (A992)	Braced frame geometry		KI/r	Brace	Beam	Beam	Drift Range
		Cross-section	Cross-section	Col Spacing (mm)	Story Height (mm)		Angle $\theta$ (degree)	Design Criteria	Beam DCR	Deformation Capacity (%)
1	HSS5x5x1/2	W12X106	W12X50	4500	3000	60.9	53.1	proposed	0.94	2.66
2		W12X106	W14X38	4500	3000	60.2	53.1	w/o 1.14	0.99	2.94
3		W12X106	W16X50	4500	3000	59.4	53.1	AISC	0.99	3.45
4		W12X120	W14X38	4500	4500	85.2	63.4	proposed	0.92	10.04
5		W12X120	W12X35	4500	4500	85.7	63.4	w/o 1.14	0.97	11.57
6		W12X136	W14X74	4500	4500	85.0	63.4	AISC	0.91	7.23
7		W12X106	W14X48	6000	3000	71.0	45.0	proposed	1	6.64
8		W12X106	W12X50	6000	3000	71.8	45.0	w/o 1.14	0.94	7.41
9		W12X106	W14X74	6000	3000	71.0	45.0	AISC	0.96	5.46
10		W12X120	W12X45	6000	4500	96.2	56.3	proposed	1	12.2
11		W12X120	W14X38	6000	4500	95.6	56.3	w/o 1.14	0.92	12.83
12		W12X152	W16X89	6000	4500	94.4	56.3	AISC	0.92	6.75
13		W12X106	W14X48	9000	3000	94.8	33.7	proposed	0.89	9.99
14		W12X106	W12X45	9000	3000	95.8	33.7	w/o 1.14	0.91	11.13
15		W12X152	W16X89	9000	3000	93.2	33.7	AISC	0.94	6.24

ID	Brace Cross-section (Material Spec.)	Column (A992)	Beam (A992)	Braced frame geometry		KI/r	Brace	Beam	Beam	Drift Range
		Cross-section	Cross-section	Col Spacing (mm)	Story Height (mm)		Angle $\theta$ (degree)	Design Criteria	Beam DCR	Deformation Capacity (%)
16		W12X120	W12X45	9000	4500	117.8	45.0	Proposed	0.94	16.11
17		W12X120	W10X45	9000	4500	118.5	45.0	w/o 1.14	0.95	18.14
18		W14X193	W18X106	9000	4500	114.6	45.0	AISC	1.02	6.12
19	HSS-4x4x1/2 (A500 Gr. C)	W14X82	W12X35	4500	3000	79.2	53.1	proposed	0.86	11.63
20		W14X82	W14X26	4500	3000	78.5	53.1	w/o 1.14	0.98	12.14
21		W14X82	W14X48	4500	3000	78.5	53.1	AISC	1	7.01
22		W14X82	W10X26	4500	4500	111.7	63.4	proposed	0.91	24.9
23		W14X82	W12X19	4500	4500	110.9	63.4	w/o 1.14	1.03	24.18
24		W12X106	W16X57	4500	4500	110.2	63.4	AISC	0.86	13.39
25		W14X74	W12X35	6000	3000	93.9	45.0	Proposed	0.86	14.18
26		W14X74	W14X26	6000	3000	93.2	45.0	w/o 1.14	0.99	15.43
27		W12X106	W14X68	6000	3000	93.5	45.0	AISC	0.92	9.72
28		W12X96	W10X26	6000	4500	126.2	56.3	Proposed	0.97	29.16
29		W12X96	W12X22	6000	4500	125.3	56.3	w/o 1.14	0.92	28.92
30		W12X136	W16X77	6000	4500	123.4	56.3	AISC	0.93	13.29
31		W14X82	W10X30	9000	3000	126.2	33.7	Proposed	0.85	21.98

ID	Brace Cross-section (Material Spec.)	Column (A992)	Beam (A992)	Braced frame geometry		KI/r	Brace	Beam	Beam	Drift Range
		Cross-section	Cross-section	Col Spacing (mm)	Story Height (mm)		Angle $\theta$ (degree)	Design Criteria	Beam DCR	Deformation Capacity (%)
32		W14X82	W10X26	9000	3000	126.5	33.7	w/o 1.14	0.88	> 16 <sup>23.16</sup>
33		W14X132	W16X77	9000	3000	121.9	33.7	AISC	0.93	11.6
34		W12X106	W12X22	9000	4500	153.6	45.0	Proposed	0.97	> 16 <sup>30.9</sup>
35		W12X106	W12X19	9000	4500	153.6	45.0	w/o 1.14	1.01	> 16 <sup>31.8</sup>
36		W14X176	W16X100	9000	4500	150.4	45.0	AISC	1	14.6
37	HSS-6x6x1/2 (A500 Gr. C)	W12X136	W14X53	4500	3000	47.4	53.1	Proposed	1	2.44
38		W12X136	W14X48	4500	3000	47.4	53.1	w/o 1.14	0.97	2.86
39		W12X136	W16X57	4500	3000	46.6	53.1	AISC	0.93	2.45
40		W12X152	W14X53	4500	4500	67.2	63.4	Proposed	0.94	2.91
41		W12X152	W14X48	4500	4500	67.2	63.4	w/o 1.14	0.91	2.98
42		W12X152	W14X74	4500	4500	67.2	63.4	AISC	0.96	3.17
43		W12X120	W18X55	6000	3000	55.0	45.0	Proposed	0.99	2.52
44		W12X120	W18X50	6000	3000	55.0	45.0	w/o 1.14	0.96	2.5
45		W12X120	W18X65	6000	3000	55.0	45.0	AISC	1.01	2.52
46		W12X152	W18X55	6000	4500	74.7	56.3	Proposed	0.94	2.81
47		W12X152	W16X50	6000	4500	75.2	56.3	w/o 1.14	0.98	3.23

ID	Brace Cross-section (Material Spec.)	Column (A992)	Beam (A992)	Braced frame geometry		KI/r	Brace	Beam	Beam	Drift Range
		Cross-section	Cross-section	Col Spacing (mm)	Story Height (mm)		Angle $\theta$ (degree)	Design Criteria	Beam DCR	Deformation Capacity (%)
48		W14X159	W18X86	6000	4500	74.2	56.3	AISC	0.93	2.94
49		W12X120	W14X68	9000	3000	74.9	33.7	Proposed	0.97	5.64
50		W12X120	W18X55	9000	3000	73.2	33.7	w/o 1.14	0.9	4.74
51		W14X159	W16X100	9000	3000	73.8	33.7	AISC	0.92	4.13
52		W12X152	W18X60	9000	4500	92.2	45.0	Proposed	0.91	6.48
53		W12X152	W18X50	9000	4500	92.2	45.0	w/o 1.14	0.97	7.34
54		W14X211	W18X119	9000	4500	91.6	45.0	AISC	0.99	4.62
55		HSS-7x7x1/2 (A500 Gr. C)	W12X152	W16X57	4500	3000	38.4	53.1	Proposed	0.96
56	W12X152		W14X53	4500	3000	39.0	53.1	w/o 1.14	1	2.97
57	W12X152		W14X53	4500	3000	38.4	53.1	AISC	0.97	2.97
58	W12X170		W16X57	4500	4500	55.1	63.4	Proposed	0.97	2.39
59	W12X170		W16X50	4500	4500	55.1	63.4	w/o 1.14	1	2.35
60	W12X170		W14X74	4500	4500	55.5	63.4	AISC	1	2.55
61	W12X152		W14X82	6000	3000	46.6	45.0	Proposed	0.94	2.51
62	W12X152		W14X74	6000	3000	46.6	45.0	w/o 1.14	0.91	2.52
63	W12X152		W16X77	6000	3000	46.1	45.0	AISC	0.96	2.52

ID	Brace Cross-section (Material Spec.)	Column (A992) Cross-section	Beam (A992) Cross-section	Braced frame geometry		KI/r	Brace Angle $\theta$ (degree)	Beam Design Criteria	Beam DCR	Drift Range Deformation Capacity (%)
				Col Spacing (mm)	Story Height (mm)					
64		W12X170	W16X77	6000	4500	62.5	56.3	Proposed	0.92	2.41
65		W12X170	W16X67	6000	4500	62.6	56.3	w/o 1.14	0.93	2.38
66		W14X176	W16X100	6000	4500	62.1	56.3	AISC	0.93	2.53
67		W12X152	W16X89	9000	3000	60.1	33.7	Proposed	0.86	2.48
68		W12X152	W16X77	9000	3000	60.1	33.7	w/o 1.14	0.88	2.36
69		W14X159	W16X100	9000	3000	59.9	33.7	AISC	0.96	2.51
70		W12X170	W16X89	9000	4500	77.6	45.0	Proposed	0.93	2.68
71		W12X170	W16X77	9000	4500	77.6	45.0	w/o 1.14	0.95	2.62
72		W14X233	W18X130	9000	4500	76.5	45.0	AISC	0.97	2.51
73		HSS- 10x10x5/8 (A500 Gr. C)	W14X283	W14X68	4500	3000	23.3	53.1	Proposed	0.94
74	W14X283		W16X57	4500	3000	22.9	53.1	w/o 1.14	0.89	3.58
75	W14X283		W14X68	4500	3000	23.3	53.1	AISC	0.94	3.59
76	W14X311		W16X77	4500	4500	33.8	63.4	Proposed	1.02	3.09
77	W14X311		W16X77	4500	4500	33.8	63.4	w/o 1.14	0.91	3.22
78	W14X311		W16X77	4500	4500	33.8	63.4	AISC	1.02	3.09
79	W14X257		W18X97	6000	3000	28.1	45.0	Proposed	0.92	2.92

ID	Brace Cross-section (Material Spec.)	Column (A992)	Beam (A992)	Braced frame geometry		KI/r	Brace	Beam	Beam	Drift Range
		Cross-section	Cross-section	Col Spacing (mm)	Story Height (mm)		Angle $\theta$ (degree)	Design Criteria	Beam DCR	Deformation Capacity (%)
80		W14X257	W16X89	6000	3000	28.4	45.0	w/o 1.14	0.99	3.01
81		W14X257	W18X97	6000	3000	28.1	45.0	AISC	0.92	2.92
82		W14X311	W18X119	6000	4500	39.2	56.3	Proposed	0.93	2.92
83		W14X311	W18X97	6000	4500	39.2	56.3	w/o 1.14	1.01	2.95
84		W14X311	W18X119	6000	4500	39.2	56.3	AISC	0.94	2.92
85		W14X233	W18X130	9000	3000	37.0	33.7	Proposed	0.94	2.88
86		W14X233	W18X119	9000	3000	37.0	33.7	w/o 1.14	0.91	3.13
87		W14X233	W18X130	9000	3000	37.0	33.7	AISC	0.94	2.88
88		W14X283	W18X158	9000	4500	49.8	45.0	Proposed	,99	2.47
89		W14X283	W18X143	9000	4500	49.8	45.0	w/o 1.14	0.96	2.45
90		W14X342	W18X192	9000	4500	49.6	45.0	AISC	0.91	2.53
91		HSS-7x7x5/8 (A500 Gr. C)	W14X193	W18X65	4500	3000	37.1	53.1	Proposed	0.93
92	W14X193		W18X55	4500	3000	37.1	53.1	w/o 1.14	0.97	4.35
93	W14X193		W18X65	4500	3000	37.1	53.1	AISC	0.93	4.07
94	W14X211		W18X65	4500	4500	53.8	63.4	Proposed	0.95	3.06
95	W14X211		W18X55	4500	4500	53.9	63.4	w/o 1.14	0.99	3.05

ID	Brace Cross-section (Material Spec.)	Column (A992)	Beam (A992)	Braced frame geometry		KI/r	Brace	Beam	Beam	Drift Range
		Cross-section	Cross-section	Col Spacing (mm)	Story Height (mm)		Angle $\theta$ (degree)	Design Criteria	Beam DCR	Deformation Capacity (%)
96		W14X211	W16X77	4500	4500	54.2	63.4	AISC	1.01	3.71
97		W14X176	W16X89	6000	3000	45.5	45.0	Proposed	0.91	2.75
98		W14X176	W16X77	6000	3000	45.5	45.0	w/o 1.14	0.93	3.09
99		W14X176	W16X89	6000	3000	45.5	45.0	AISC	0.99	3.09
100		W14X193	W16X89	6000	4500	62.2	56.3	Proposed	0.94	2.41
101		W14X193	W16X77	6000	4500	62.2	56.3	w/o 1.14	0.96	3.14
102		W14X193	W18X106	6000	4500	61.8	56.3	AISC	0.97	3.23
103		W14X159	W16X100	9000	3000	60.0	33.7	Proposed	0.91	2.48
104		W14X159	W16X89	9000	3000	60.2	33.7	w/o 1.14	0.9	3.11
105		W14X176	W18X106	9000	3000	59.4	33.7	AISC	1.02	2.94
106		W14X193	W16X100	9000	4500	78.8	45.0	Proposed	0.96	2.67
107		W14X193	W16X89	9000	4500	78.8	45.0	w/o 1.14	0.97	3.11
108		W14X257	W18X158	9000	4500	77.9	45.0	AISC	0.96	2.58
109		HSS-3x3x3/8 (A500 Gr. C)	W12X50	W10X17	4500	3000	110.4	53.1	Proposed	0.82
110	W12X50		W8X15	4500	3000	111.5	53.1	w/o 1.14	0.96	> 16 <sub>20</sub>
111	W14X53		W10X45	4500	3000	109.3	53.1	AISC	0.95	11.8



## 4.2 Seismic Response-History Analysis of 3 and 9-Story Chevron SCBFs

The analysis proposed with this study consisted of an inelastic parameter study described above. However, the parameter analysis investigates nonlinear behavior, but the cyclic deformations are not directly related to seismic response to earthquake excitations. As a result, a limited study of inelastic dynamic response of chevron braced frames with yielding beams to equations was added to provide a measure of the type of story drifts that may be expected with earthquake accelerations of this system and other comparable braced frames.

Both 3- and 9-story buildings were designed, and the modeling approach presented in Chapter 3 was used to conduct seismic response-history analysis. The building geometries are shown in Fig. 4-1. Three different designs were used for each different building heights (comprising two sets of designs, one for the three-story geometry and one set of the 9-story geometry) including: (1) chevron meeting current AISC SCBF provisions, (2) chevron with yielding beams using the proposed design philosophy and (3) a multi-story X meeting current AISC SCBF provisions. All 6 frames were designed for seismic forces using the Equivalent Lateral Force (ELF) procedure in ASCE 7-16 (ASCE 2016) for a location in Seattle, WA. The braced bays were placed at the perimeter of the building in both directions, as illustrated in the figure.

The seismic design spectrum defined by ASCE 7-16 (ASCE 2016) was developed using the following values:  $S_{DS}$  of 0.94g and an  $S_{D1}$  of 0.48g for the Seattle location on Site Class C soil. The seismic response-modification coefficient,  $R$ , of 6 and an occupancy importance factor of 1.0 were used. The building geometry, gravity loads and mass for floor and roof levels were as defined for the buildings in the SAC Steel Project.

The braces were A500 Gr. C rectangular hollow structural sections. All beams and columns used A992 Gr. 50 wide-flange sections. The braces were welded to the gusset plates, and beam-to-column connections were welded-flange-welded-web connections except that single-plate shear connections were used for top story in chevron configurations and every other story for the X-brace system where no corner gusset was present.

The buildings designated as “Proposed” were designed using the proposed design method using the full plastic capacity of the beams and the 1.14 factor in  $P_{cre}$  discussed in the previous section. The “AISC” chevrons and multi-story X buildings were designed based on the load cases specified in the Seismic Provision. The columns were designed for the accumulated expected brace forces for the “AISC” design with the same columns were used for each set of buildings to avoid

any bias in the performance that would be provided by the contribution of the columns to lateral strength. The column size was either that required to meet the Seismic Design Provisions or to have the columns meet the strong column-weak beam requirements for the beam sizes in the proposed chevron designs. The gusset plate connections were designed using an elliptical clearance and the balance design philosophy to permit secondary yielding in the gusset plate connection (Roeder et al. 2011). Tables 4-2 and 4-3 list all the brace, beam and column section sizes for 3-story, 9-story chevron and multi-story X-braced frames, respectively.

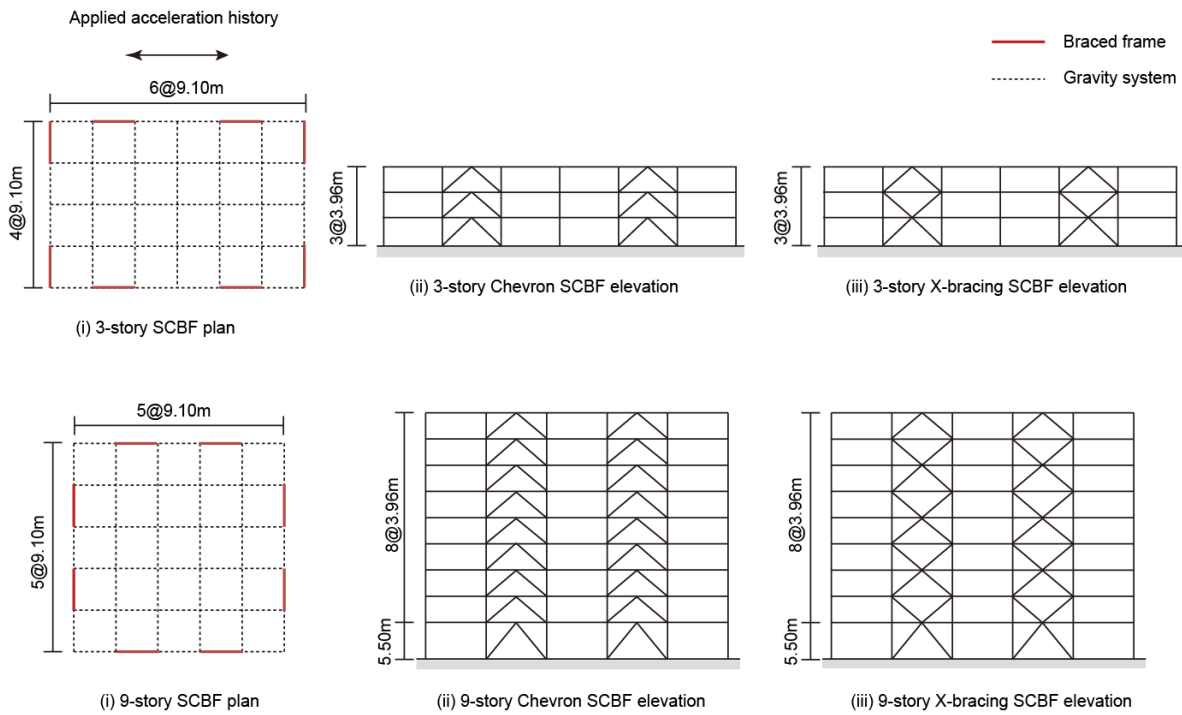


**Figure 4-1. Three-story and nine-story archetype SCBFs: (a) three-story and (b) nine-story buildings**

**Table 4-2. Three-story archetype member sizes**

Story	Column	Brace	Beam		
			Proposed chevron	AISC chevron	X-bracing
1	W14×82	HSS6×6×1/2	W18×65	W24×103	W14×38
2	W14×82	HSS5×5×1/2	W14×53	W24×94	W14×38
3	W14×82	HSS4 <sup>1</sup> / <sub>2</sub> ×4 <sup>1</sup> / <sub>2</sub> × <sup>3</sup> / <sub>8</sub>	W18×65	W24×146	W24×146

**Table 4-3. Nine-story archetype member sizes**

Story	Column	Brace	Beam		
			Proposed chevron	AISC chevron	X-bracing
1	W14×283	HSS7×7× <sup>5</sup> / <sub>8</sub>	W24×84	W24×146	W24×62
2	W14×283	HSS6×6× <sup>5</sup> / <sub>8</sub>	W21×68	W24×131	W18×55
3	W14×283	HSS6×6× <sup>5</sup> / <sub>8</sub>	W21×68	W24×131	W18×55
4	W14×193	HSS6×6× <sup>5</sup> / <sub>8</sub>	W21×68	W24×131	W18×55
5	W14×193	HSS6×6× <sup>1</sup> / <sub>2</sub>	W18×65	W24×94	W18×55
6	W14×193	HSS6×6× <sup>1</sup> / <sub>2</sub>	W18×65	W24×94	W18×55
7	W14×74	HSS6×6× <sup>1</sup> / <sub>2</sub>	W18×65	W24×94	W18×55
8	W14×74	HSS5×5× <sup>3</sup> / <sub>8</sub>	W14×48	W21×83	W18×55
9	W14×74	HSS5×5× <sup>3</sup> / <sub>8</sub>	W21×68	W24×146	W24×146

The systems were modeled with the OpenSees computer program consider yielding of the beams and columns and buckling, tensile yielding, post-buckling deformation, brace fracture and deformations after brace as used in the parameter study models and briefly summarized in sections 3.3 and 3.4. In addition to the general braced frame modeling, the second-order effects of the gravity system were included using a leaning (P-delta) column. Previous research has shown that the gravity frame can resist a portion of the seismic loads, therefore the models used here include non-linear rotational springs that account for the gravity frame’s shear-plate moment resisting capacity using the model proposed by Liu et al. (Liu et al. 2004).

Two suites of ground motions were selected from the NGAWest2 Database (Ancheta et al. 2014). These record suites are targeted to the 10% and 2% probability of exceedance in 50 years Uniform Hazard Spectra (UHS) obtained from the USGS hazard maps [USGS 2016] for the site of the structure. Each suite contains 30 pairs of ground motions (60 horizontal components) which were scaled to minimize the weighted error between the UHS and geometric-mean spectral accelerations. The periods of the first mode were calculated for all systems, and these periods were used in the scaling process. Figure 4-2 shows the target UHS and geometric mean of the scaled spectra for each suite of ground motions. The error was evaluated between  $0.5T_1$  and  $5T_1$  with

maximum weight at  $T_1$  and logarithmically decaying weight to the period bounds. The period bounds were chosen to ensure the ground motions were sufficiently intense at shorter periods corresponding to higher modes and elongated periods corresponding to post-brace-buckling and brace-fracture structural performance states. The same sets of ground motions were used for both 3- and 9-story buildings. No more than 2 records were picked up from the same event and all scale factors were less than 5.0.

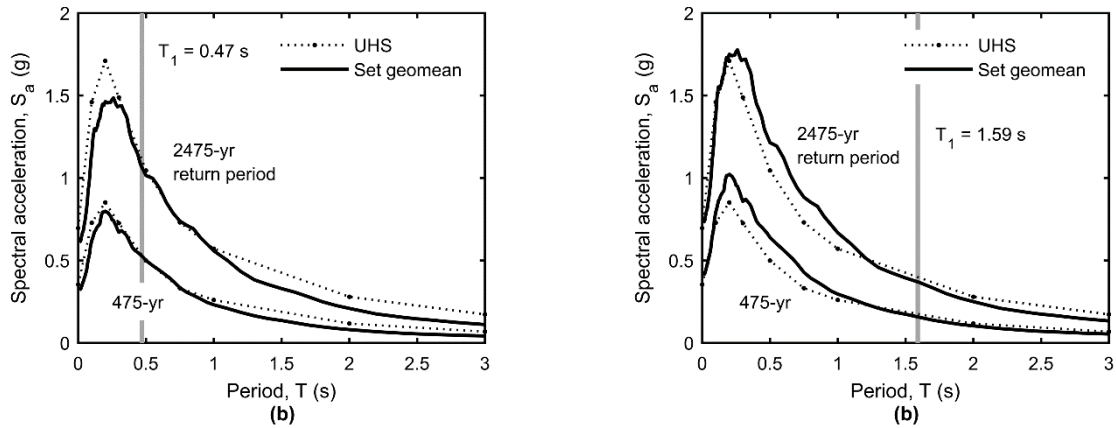


**Figure 4-2. Target UHS spectra and scaled spectra of the selected ground motion suites for: (a) three-story buildings, and (b) nine-story buildings**

The maximum story drifts (one direction only, not drift range) for all stories of all 3 and 9 story frames are shown in Fig. 4-3. The 9-story frames had smaller drift levels than 3-story frames for all designs as shown in prior research (Hsiao et al 2013b). Again, the distribution of drift for 9-story frames is more uniform in the proposed chevron than the AISC chevron, and the median maximum story drift for the proposed chevron is slightly smaller than that for AISC chevron and X-braced designs. However, unlike for the 3-story frames, the difference in the 84<sup>th</sup> percentile responses for the three designs was small. This is to be expected since the drift of 9-story frames are more influenced by global overturning than the 3-story frames and the column sizes between the three designs are the same.

It should also be noted that the median maximum story drift for all designs for both building heights are less than 2% in the 2% in 50-year hazard level. The same is true for the 84<sup>th</sup> percentile values for the 10% in 50-year hazard. This indicates that the Proposed chevron frames meet or exceed the seismic performance expectations for braced frames.

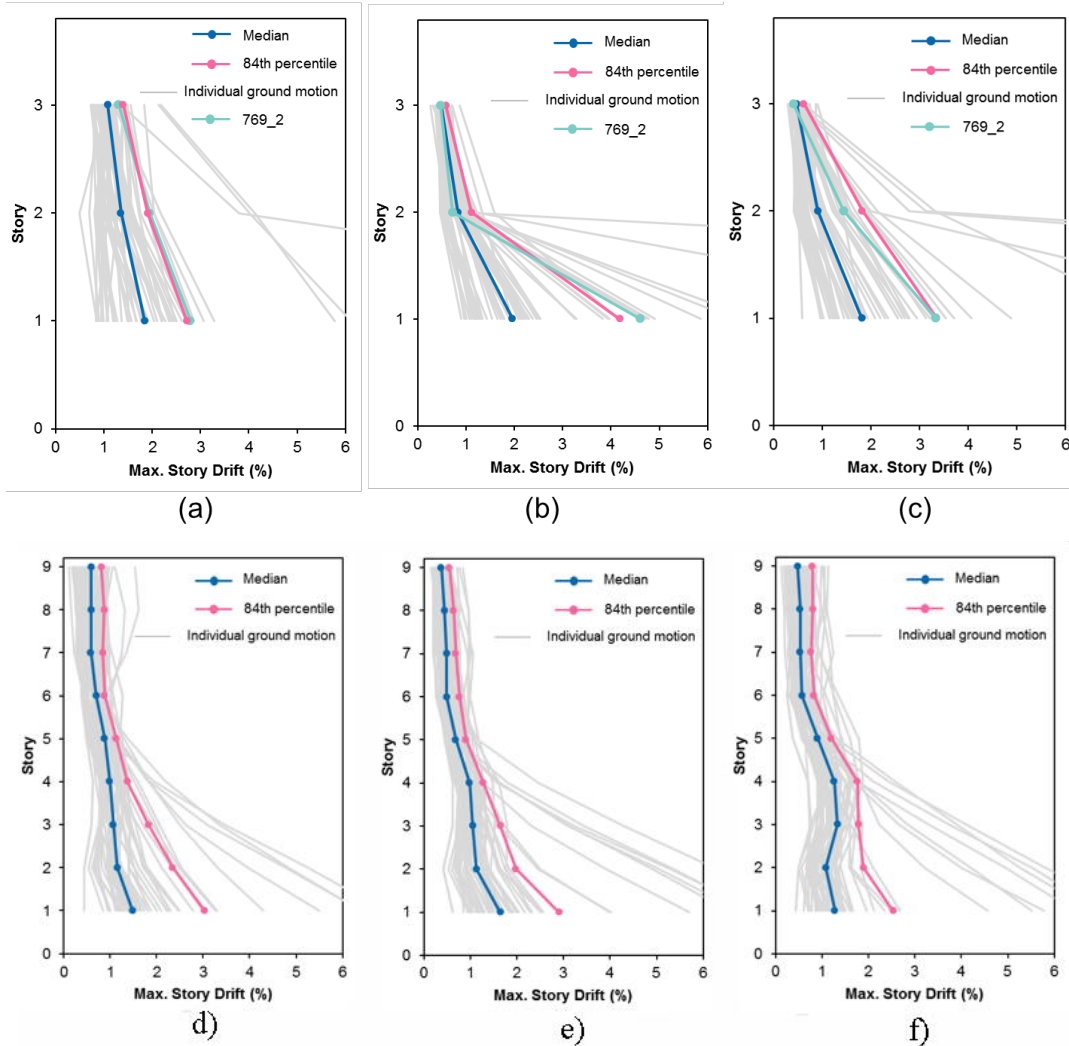


**Figure 4-3 Maximum drift on each story for all buildings for the 2% in 50 year hazard level: (a) 3 story proposed chevron; (b) 3 story AISC chevron; (c) 3 story X-braced d) 9 story proposed chevron; e) 9 story AISC chevron f) 9 story X-braced**

Statistical analyses of the computed story drifts were performed, and these analyses show that the computed median maximum story drifts are approximately 4% larger for chevron braced frames designed by the current AISC SCBF procedure than for chevrons designed by the proposed method. X-braced frames have median maximum story drifts that were slightly smaller than both chevron systems. The story drifts are more uniformly distributed over height with the proposed chevron system than either the SCBF chevron or X-braced systems.

The occurrence of several structural performance states were considered in evaluating the seismic performance of the braced frames associated with the servicability, repair and collapse prevention performance objectives. Brace fracture is predicted with reasonable accuracy in the

OpenSEES model with the calibrated Maximum Strain Range model described in Section 3. Collapse is not easily or accurately predicted, but collapse was postulated as occurring for analyses with numerical instability and for predicted story drifts larger than 8%. The 8% limit was selected because there is no physical evidence to suggest that braced frames can retain their connections and structural integrity for larger drift levels. Beam deflections are not a safety issue, but they are of interest with respect to repair of damage after major earthquakes, and they are accurately computed from the analyses. Figure 4-4 shows the percentage of the ground motions for each frame type at each hazard level that resulted in: (i) vertical beam deflections  $\delta$  in excess of  $L/100$  in any story, (ii) vertical beam deflection  $\delta$  in excess of  $L/50$  in any story, (iii) at least one brace to fracture, and (iv) potential collapse indicated by exceeding 8% story drift at any story.

The proposed chevron designs consistently had lower percentages of brace fracture and potential collapse. The differences in the frequency of occurrence of these two damage states is particularly striking. For the 3-story frames, the AISC chevron and X-braced frames had brace fracture in over 40% of the 2% in 50 year ground motions while the Proposed Chevron had brace fracture in fewer than 20% of those ground motions. Similarly, for the 10% in 50-year ground motions, there were no occurrences of brace fracture for the Proposed Chevron while brace fracture occurred in 5% of the ground motions for both the AISC Chevron and X-Braced frames. Notably, all frames had less than 10% probability of collapse in the 2% in 50 year hazard level, which is an approximate target for new buildings designed per ASCE 7-16. Collapse probabilities were smaller for the Proposed Chevron.

The trade-off for improved brace fracture and collapse performance is increased vertical deformation of the chevron beam in the Proposed Chevron frames. For the 3-story frame (Fig. 4-4) there were no occurrences of beam deflection exceeding  $L/100$  in the 10% in 50 years hazard level ground motion suite, however, 20% of the ground motions caused that level of beam deformation in the 2% in 50 years hazard level for the Proposed Chevron.

Figure 4-5 shows the results for the nine-story buildings. Compared to the 3-story buildings, smaller percentage of both brace fracture and collapse were observed, while the probabilities of beam deflection exceeding  $L/100$  and  $L/50$  are slightly larger.

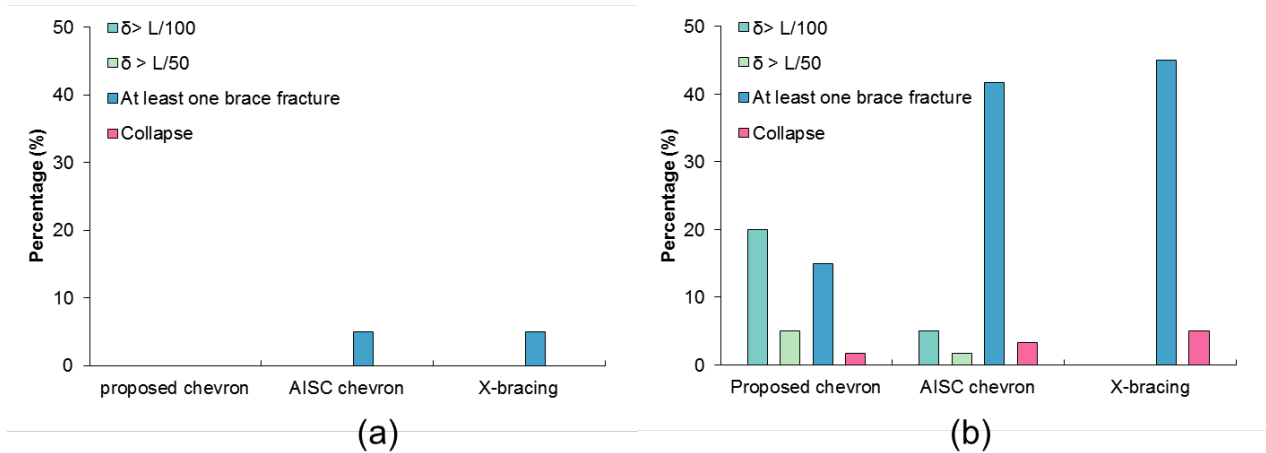


**Figure 4-4. Percentage of ground motions causing selected damages states: (a) 3 story 2% in 50-year hazard, b) 9 story 2% in 50-year hazard.**

The nonlinear response history analyses showed that for the 10% in 50-year hazard level the response of the Proposed Chevron SCBF was better than that of AISC chevron SCBFs designed using current AISC Seismic Provisions and for X-braced SCBFs. This assessment of performance was true for story drift and the occurrence of brace fracture for both the three- and nine-story buildings. Moreover, even though the proposed design allows moderate beam yielding, the beam deflections for the 10% in 50-year hazard level were not large, and only one ground motion resulted in a beam deflection exceeding 1% of the beam length. For the 2% in 50 year hazard level, the nonlinear time history analyses demonstrated that the Proposed Chevron SCBFs had fewer instances of brace fracture and generally smaller story drifts relative to the chevron braced frames and X-braced SCBFs designed to the current AISC Seismic Provisions. The beam yielding limited the tensile deformation of the brace and increased the drift at which brace fracture occurs, as observed in the previous experimental studies.

## Chapter 5 Detailed Analysis of Parameter Study Results

The results presented in Chapter 4 were analyzed to determine the influence of salient study parameters. This chapter presents that analysis.

### 5.1 Global Brace Slenderness Ratio

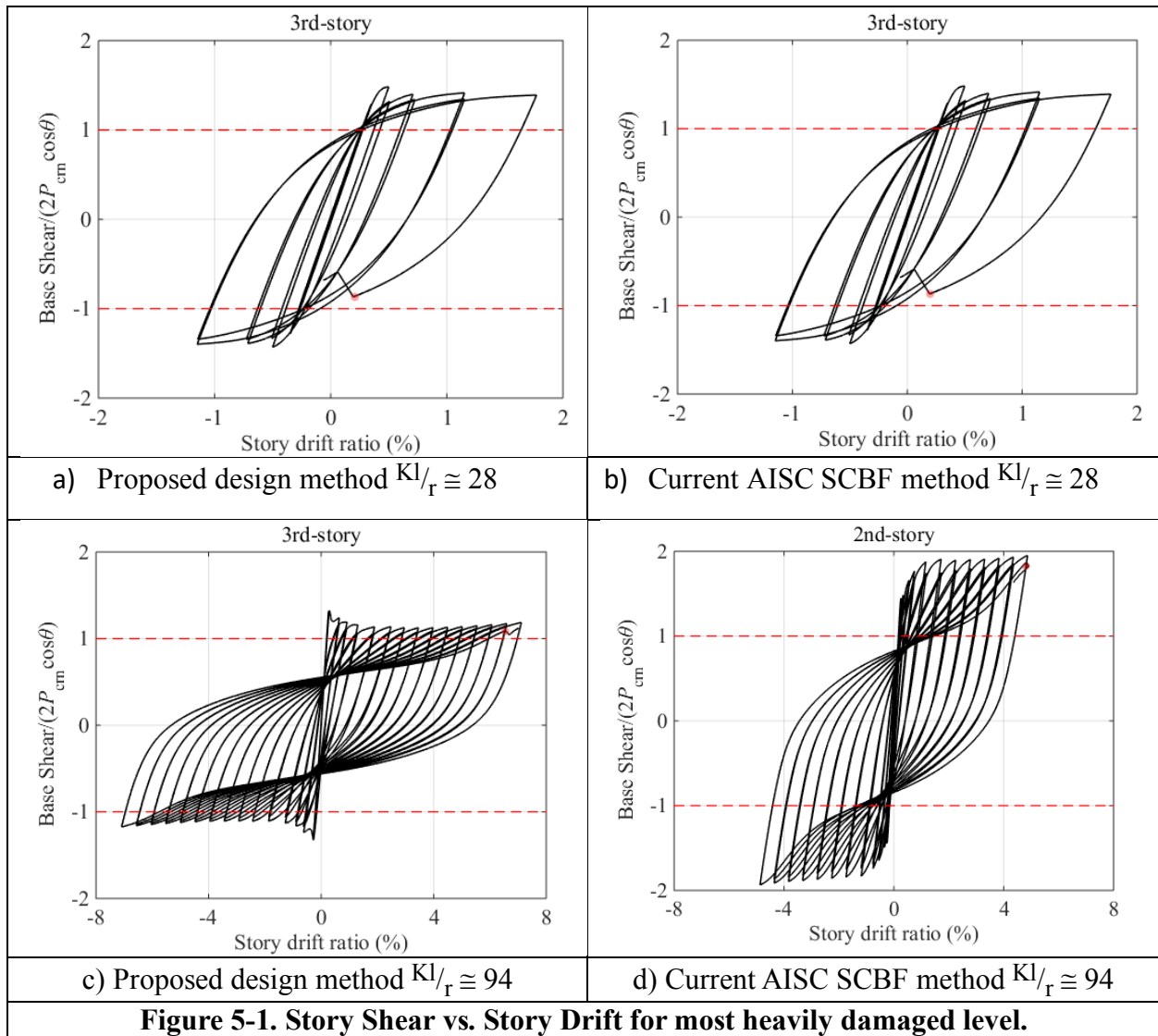
Analysis of the data in Table 4-1 demonstrates that it is the variation in  $Kl/r$  is the most influential parameter in this evaluation. The parameter,  $Kl/r$ , was varied between 28 and 154 in these analyses. This range effectively covers the full range that can be expected in practice, and Fig. 5-1 shows the effect of this variation (for  $Kl/r = 28$  and  $Kl/r = 94$ ). As shown in this figure, the difference between the proposed design method and the current AISC SCBF method is negligible for small  $Kl/r$  values. The two design methods are distinguished by the difference between  $P_{ye}$  and  $P_{cre}$ , and this difference is very small for low values of  $Kl/r$ . Therefore, the two design methods have the same chevron beam sizes under this condition, and inelastic deformation achieved under this condition are very small as shown in Fig. 5-1a and b. The difference between  $P_{ye}$  and  $P_{cre}$  is large for large values of  $Kl/r$ .

Larger values of  $Kl/r$  result in significantly smaller beams and dramatically increased inelastic deformation capacity for frames designed with the proposed method. With the proposed yielding beam design procedure, a drift range of over 15% is achieved prior to brace fracture, while with the current design requirements the drift range is just over 9% at brace fracture. Intermediate values of  $Kl/r$ , i.e., those between 65 and 120 show the largest increase in drift capacity before brace fracture with the proposed design method. The figure and data in Table 4-1 clearly show that chevron braced frames with more slender braces designed by the proposed method achieve larger inelastic deformations prior to brace fracture than other braced frame systems.

The transition between slender and stocky braces is not easily determined from Table 4-1, but the drift range of about 5% to 6% represents the approximate transition between very good braced frame performance and reduced performance. Further, the issue is complicated by the local slenderness,  $b/t$  ratio, since this local slender varied widely with brace size. For braces that clearly met current local slenderness limits and values greater than 65 showed large inelastic deformations

prior to brace frame and significant increases in inelastic deformation prior to brace fracture with the proposed design method.

Figure 5-1 also shows that regardless of the  $Kl/r$  value, frames designed by the proposed method developed the full design lateral resistance,  $2P_{cm}\cos\theta$ , and retained that resistance through significant inelastic deformation. Frames with braces at the current SCBF highly ductile slenderness limit for rectangular HSS braces achieved limited deformation capacity regardless of the design method.



## 5.2 Brace Angle

The influence of the angle of inclination of the brace was also studied. The brace angle varied from approximately 34 degrees to 63 degrees, which represents the full range of practical

usage (presented in Table 4-1). Figures 5-2 and 5-3 show the results for frames with different bay widths, which result in a brace angle of approximately 63 degrees for the data shown in Figs. 5-2a and 5-3a and approximately 34 degrees for the data shown in Figs. 5-2b and 5-3b. The results show that there is not a significant difference however, it should be noted, that flatter angles may be structurally more efficient at resisting story shear. The data presented in Table 4-1 shows that for a given building height, steeper angles result in significantly smaller beams than flatter brace angles for a given brace size, because the reduced beam length reduces the bending moment demand which is critical for beam design.

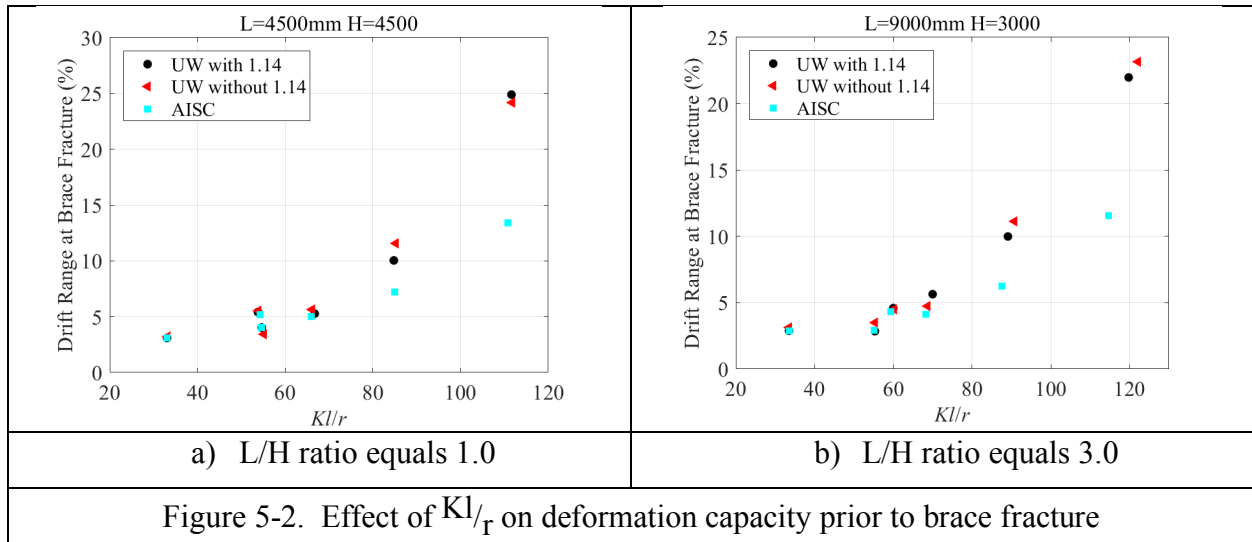


Figure 5-2. Effect of  $Kl/r$  on deformation capacity prior to brace fracture

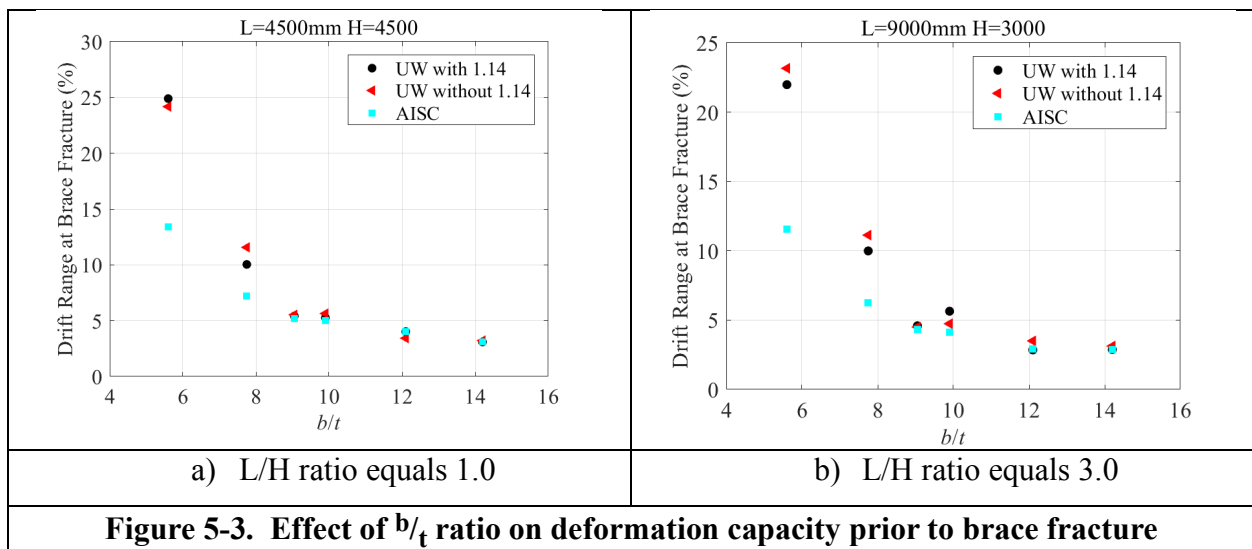


Figure 5-3. Effect of  $b/t$  ratio on deformation capacity prior to brace fracture

### 5.3 Effect on Column Axial Force

The effect of column axial force was not directly addressed in the parameter study, since all columns were designed to develop the accumulated expected brace forces as required by the 2016 AISC SCBF requirements. However, the computed axial force in the brace was monitored, and it is clear that using the proposed method can significantly reduce the axial forces in the column. However, this reduction is only achieved when there is significant yielding in the beam.

For the frames in this study regardless of the design method (current AISC or proposed), the beams were designed to be the minimum size required to meet the design loads. A plastic analysis of each beam was performed, using one of the mechanisms shown in Fig 5-4. Engineers are conservative when designing members and might assume that if a W24x96 meets the design minimum, a larger member, i.e., a W24x104, will be even better. However, this is not the case because, as demonstrated here, additional yielding of the beam will increase the drift capacity of the building and this yielding will not occur if the beam is oversized.

In addition to inherent conservatism, engineers may also want to avoid the plastic approach for simplicity of design and possibly distrust of the procedure. Again, if the plastic mechanism is not considered, the design will result in chevron beams that are larger than required. As a result, it recommended that we retain the current column axial loads with this proposed design method.

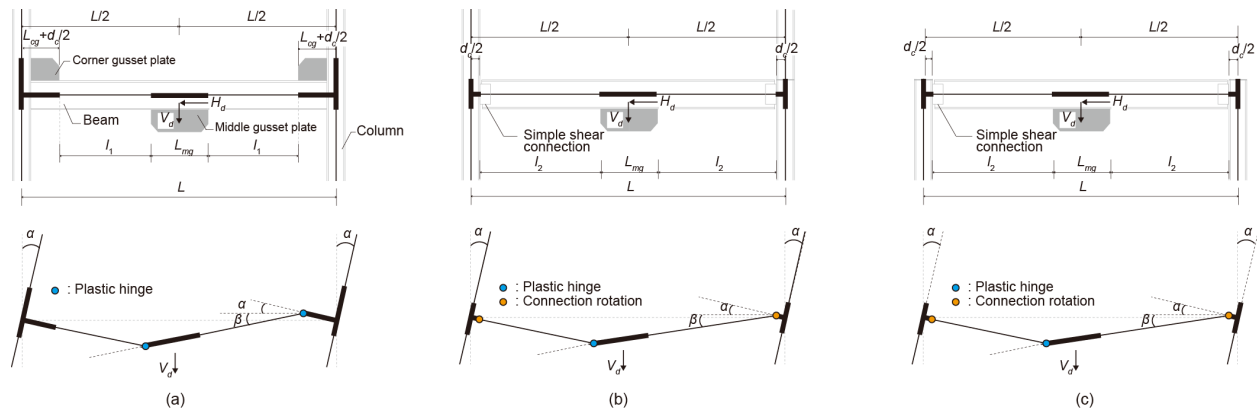


**Figure 5-4. Beam geometry and plastic mechanisms: (a) chevron beam restrained with corner gusset plates, (b) and (c) chevron beam restrained without corner gusset plate and having simple shear connections for middle or top story respectively.**

### 5.4 Axial Force on the Beam

Initially, the proposed design recommended that the beam be designed so the axial stress due to axial loads by the chevron beam load states did not exceed  $0.5F_y$ . This recommendation was made because the axial load the braces transfer to the beam are not reduced by flexural yielding.

In additions, ABAQUS analyses performed showed a change in behavior with high axial stress demands with very weak beams.

However, this recommendation is not carried forward, because it is quite difficult to get a beam to this large axial stress level, because compressive and tensile stress limits prevent keep stress below  $0.6 F_y$ . The application of resistance factors further limits the actual stress in the beam. Hence, the limit seems somewhat redundant for practical design. Finally, in the design of the 111 frames for this parameter study, only two beams exceeded the  $0.5F_y$  limit. Neither of these two frames behaved particularly well, but the behavior does not appear to be caused by the beam axial stress demands. Both frames had very low  $Kl/r$  values and high  $b/t$  values, and these slender limits appear to have much more dominant effects. As such this limit is not included in the proposed design method.

### **5.5 Effect of Different Beam-Column Connections and Beam-Column Strength Ratio**

Alternate beam-column connections were not analyzed with the OpenSees computer program, because this program is not well suited for simulating the local behavior associated with connections. However, during this study alternate connections were analyzed with the nonlinear ABAQUS computer program. These ABAQUS analysis indicated that welded-flange-bolted-webs will perform as well as the welded-flange-welded web connections at corner gusset plates, if the connection is properly evaluated for axial-load transfer. The welded-flange-welded-web beam-column connection was used in this research on recommendations of practicing engineers on the advisory committee.

The ABAQUS connection was used also to evaluate the moment-release connection where the beam web is bolted to an integral gusset plate to release beam moments at the beam-column connection. This connection is not recommended for use with the chevron yielding beam concept. First, the moment release means the yielding beam must be treated as a simple span beam, and the yielding concept has significantly reduced benefits under that condition. Second, the lateral and lateral-torsional stability of the beam is important because of the beam yielding and the out-of-plane forces the buckled brace place on the bottom flange of the beam. Further, the lateral torsional restraint at the released ends of the beam are significantly reduced, and analysis suggest that end release is not a particularly good concept for chevrons with yielding beams.

## 5.6 Beam Deflections

In Phase I and II of the research, it was frequently noted that beam deflections occur both for chevrons designed by the current AISC SCBF method and for the proposed design method for yielding beams. It was also noted that the vertical deflections of the beam are not extremely large even with the proposed beam yielding method. Figure 5-5 shows the maximum computed beam deflection for braces with small and large angles of inclination at 2% story drift. The deflections are normalized by the clear beam span length. The deflections are the maximum deflection at 2% story drift. It can be seen that beam deflections occur even with the current AISC SCBF procedure, but maximum deflections are still quite modest, since Figure 5-3 shows that a 2% story has less a 50% chance of occurring even in 2500-year earthquake.

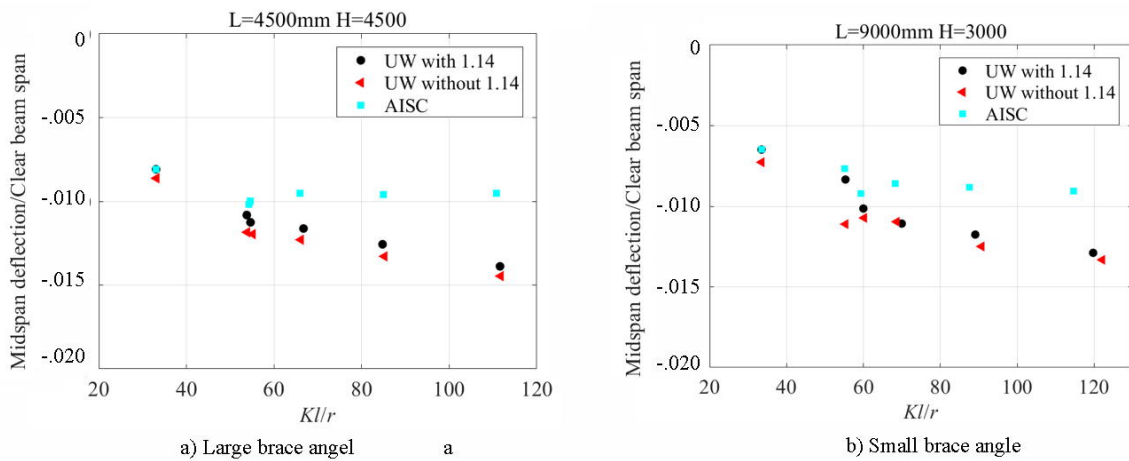


**Figure 5-5. Normalized maximum beam deflections at 2% story drift**

## Chapter 6 Summary and Conclusions

### 6.1 Summary

This report summarizes Phase III of a comprehensive research study on the effect of yielding beams in chevron braced frames. Phases I and II were largely experimental studies which showed that chevron braced frames with controlled beam yielding may actually improve the seismic performance of chevron braced frames. The yielding beams may result in a significant reduction in chevron beam size, and the beam yielding may significantly increase the deformation capacity of the braced frame prior to brace fracture. This occurs because the downward deflection of the beam reduces the tensile force in the brace during post buckling deformation, and the reduced tensile force reduces the tensile plastic strain in the buckled region of the brace and delays brace fracture. Inelastic beam deflections occur with yielding beams but the deflections noted at deformations commonly Nonlinear finite element analysis performed as part of Phase I and II support these experimental observations.

The Phase I and II research focused on braces inclined at 45 degrees with intermediate slenderness ratios. This Phase III research was an analytical study to examine the ramifications of the proposed design method through the full range of possible structural designs. To evaluate the global goals, seven brace sizes were analyzed (HSS3x3x<sup>3</sup>/<sub>8</sub>, HSS4x4x<sup>1</sup>/<sub>2</sub>, HSS5x5x<sup>1</sup>/<sub>2</sub>, HSS6x6x<sup>1</sup>/<sub>2</sub>, HSS7x7x<sup>1</sup>/<sub>2</sub>, HSS7x7x<sup>5</sup>/<sub>8</sub>, and HSS10x10x<sup>5</sup>/<sub>8</sub>). These brace sizes run from very compact to slightly noncompact. The column spacing story height of the baseline frame were 6000mm (19.7 ft) and 3059mm (20.0 3 ft). These dimensions were controlled by the Taiwan test setup. However, column spacings of 4500 mm (14.75 ft) and 9000 mm (29.5 ft) were also analyzed. A total 111 3 story frames with 37 combinations where one frame was designed as a chevron with the proposed yielding beam method, another was designed by the yielding beam criteria without the 1.14 in the determination of the expected buckling force, and a third was a chevron design by the current AISC SCBF criteria for each of the 37 brace and geometry combinations.

In addition, a limited dynamic time-history analysis study was performed to address the expected seismic performance of chevron braced frames compared to other braced frame systems, Three- and nine-story braced frames were designed by the proposed criteria for chevron braced

frames with yielding beams, X-braced frames, and chevron braced frames by the current AISC SCBF design criteria. Dynamic analyses were performed using a suite of acceleration records scaled to the 10% in 50-year hazard level and 2% in 50-year hazard level were performed.

## 6.2 Conclusions

This research supports the conclusions of the prior Phase I and Phase II research. Chevron braced frames with yielding braced frames with yielding beams sustain inelastic vertical deflections during inelastic deformation. These deflections reduce the maximum tensile deformation of the brace, and as a consequence reduce the tensile yield strain on the critical buckled region of the brace thus delaying brace fracture. This results in a significantly smaller chevron beam and improved inelastic performance of the braced frame. The chevron braced frame with yielding beams will achieve inelastic deformations equal to or significantly larger than the inelastic deformation achieved by chevron braced frame by the current AISC SCBF method prior to brace fracture. Chevron braced frames with yielding beams will achieve the same nominal design resistance ( $2P_{crn}\cos\theta$ ) developed by the chevron designed by the AISC SCBF procedure, and it will retain this resistance through significant inelastic deformation. The primary design change to achieve this goal and to control the inelastic deformation is to the expected tensile of the brace for chevron beam design to the magnitude of  $P_{cre}$ .

This Phase III analysis investigated the consequences of applying these research recommendations to a wider range of member sizes and structural geometries. The results of this Phase III research show that:

1. The proposed criteria designing yielding chevron beams always provides behavior equal to or better than that provided by chevron braced frames designed by the current AISC SCBF criteria.
2. The results show a dependence on the global slenderness ratio of the brace. For braces with larger  $Kl/r$  values (70 and larger), the proposed method results in significant reduction in beam size and a significant increase in inelastic deformation capacity. For very low  $Kl/r$  values (50 and smaller), the proposed method results in identical beam sizes and identical inelastic deformation capacity provided by current AISC SCBF chevron braced frames. For intermediate  $Kl/r$  values (50 to 70), beam size may be similar or slightly smaller than

that achieved by the AISC SCBF procedure, and the deformation capacity of the proposed system will be equal or better than that of the AISC SCBF systems.

3. The inclination angle of the brace does not have a significant impact on the performance of the designed chevron braced frames.
4. The research model simulated brace fracture based upon a database of prior brace tests. There is limited test data on large braces, and so the model is somewhat suspect in that area. However, the model suggests that inelastic deformation capacity of large braces with small  $Kl/r$  values and large  $b/t$  values have very limited inelastic deformation capacity, and this appears to be true for all SCBFs, regardless of the beam design.
5. Dynamic analysis of 3- and 9-story braced frames design by proposed method chevron braced frames, the current AISC SCBF chevron braced frames, and X-braced frames. Dynamic analyses show that the proposed yielding beam chevron system will on average have 1) slightly smaller inelastic story drift than the current AISC SCBF chevron system; 2) slightly larger story drift than the X-braced system; 3) fewer fractured braces and smaller drift demands (and therefore probability of collapse) than either the current AISC SCBF chevron or the X-braced frame; and 4) somewhat larger beam deflections than the current AISC SCBF chevron or the X-braced frame.

### 6.3 Further Issues

Two further issues arise from the Phase III research. First the poor inelastic deformation capacity of the large braces with small  $Kl/r$  values and large  $b/t$  values raises a general concern. As noted earlier, the performance of chevron braced frames with yielding beams is equal to or often better than that of current SCBF designs. However, the cyclic deformation pattern used for the parameter study are not seismic excitations. The braces with small  $Kl/r$  values and large  $b/t$  values do not achieve large inelastic deformations, but perhaps they do not need to achieve large inelastic deformations. These braces may have fuller hysteresis curves with strain hardening rather than softening noted with other slender braces. Hence, they may not need as large deformations as required for other braces. A dynamic time-history analysis under a suite of earthquake excitations would provide guidance on that issue. The research team is currently starting a suite of these analyses and should have results in several months.

The fracture model is based on a large database but few tests of large braces are in that database. Additional test on large braces to better define the fracture model would be beneficial in addressing the large brace issue.

## References

AISC/ANSI 341-10 (2010) "Seismic Provisions for Structural Steel Buildings," AISC, Chicago.

ASCE 7-10 (2010) "Minimum Design Loads for Buildings and Other Structures," ASCE, Reston, VA.

Balazadeh-Minouei, Y., Koboevic, S., and Tremblay, R., (2018). "Seismic Assessment of Existing Steel Chevron Braced Frames," *Journal of Structural Engineering*, ASCE, ISSN 0733-9445.

FEMA (2000). "State of the Art Report on Systems Performance of Steel Moment Frames Subject to Earthquake Ground Shaking." FEMA-355C, Federal Emergency Management Agency, Washington, D.C.

Foutch, D. A., Goel, S. C., and Roeder, C. W. (1987). "Seismic testing of full-scale steel building—part i." *Journal of Structural Engineering*, 113(11), 2111–2129.

Fukuta, T., Nishiyama, I., Yamanouchi, H., and Kato, B. (1989). "Seismic performance of steel frames with inverted v braces." *Journal of Structural Engineering*, 115(8), 2016–2028.

Hsiao P. C., Lehman D. E., and Roeder C. W. (2012). "Improved analytical model for special concentrically braced frames." *Journal of Constructional Steel Research*, 73, 80-94.

Hsiao P. C., Lehman D. E., and Roeder C. W. (2013). "A model to simulate special concentrically braced frames beyond brace fracture." *Earthquake Engineering & Structural Dynamics*, 42, 183-200.

Lehman, D.E., Roeder, C.W., Herman, D., Johnson, S., and Kotulka, B., (2008) "Improved Seismic Performance of Gusset Plate Connections," ASCE, *Journal of Structural Engineering*, Vol.134, No. 6, Reston, VA, pgs 890-901.

Lumpkin, E. J. , 2009. *Enhanced Seismic Performance of Multi-Story Special Concentrically Braced Frames Using a Balanced Design Procedure*, MSCE thesis, University of Washington, Seattle.

Liu, J. and Astaneh-Asl, M. (2004). “Moment-rotation parameters for composite shear tab connections.” *Journal of Structural Engineering*, 130(9), 1371-1380.

Menegotto, M. and Pinto, P. E. (1973). “Method of analysis for cyclically loaded reinforced concrete plane frames including change in geometry and non-elastic behavior of elements under combined normal force and bending.” *Proceedings of the IABSE Symposium on Resistance and Ultimate Deformability of Structured Act on by Well-Defined Repeated Loads*, Lisbon.

McKenna F., Scott M. H., and Fenves G. L. (2010). “Nonlinear finite-element analysis software architecture using object composition.” *Journal of Computing in Civil Engineering*, 24(1), 95-107.

Okazaki, T., Lignos, D.G., Hikin, T., and Kajiwara, T., (2013) “Dynamic Response of a Chevron Concentrically Braced Frame,” *Journal of Structural Engineering*, ASCE, Vol 139, No 4., pgs 515-525.

Popov, E. P., “On California Structural Steel Seismic Design,” Pacific Structural Steel Conference, Auckland, New Zealand, August 1986.

Roeder, C. W. (1989). “Seismic behavior of concentrically braced frame.” *Journal of Structural Engineering*, 115(8), 1837–1856.

Roeder, C.W., Foutch, D.A. and Goel, S.C., (1987) Seismic testing of a full scale steel building - Part II, *Journal of Structural Division*, ASCE, No. ST11, Vol. 113, New York, pgs 2130-45.

Roeder, C.W., Lumpkin, E.J., and Lehman, D.E. (2011) “Balanced Design Procedure for Special Concentrically Braced Frame Connections,” Elsevier, *Journal of Constructional Steel Research*, Vol 67 No 11, pgs 1760-72.

Roeder, C.W., Sen, A.D., Asada, H., Ibarra, S.M., Lehman, D.E., Berman, J.W., Tsai, K-C, Tsai, C-Y, Wu, A-C, Wang, K-J, and Liu, R. (2019). “Seismic Performance and Design of Chevron Braced Frames with Yielding Beams,” currently under publication review, *Journal of Constructional Steel Research*, Elsevier.

Sen, Andrew. D., Roeder, Charles W., Berman, Jeffrey W., Lehman, Dawn E., Li, Choa-Hsien, Wu, An-Chien, and Tsai, Keh-Chyuan (2016a) “Experimental Investigation of Chevron Concentrically Braced Frames with Yielding Beams,” *Journal of Structural Engineering*, Vol 142, No. 12, ASCE, Reston, VA.

Sen, Andrew D., Sloat, Daniel, Ballard, Ryan, Johnson, Molly M., Roeder, Charles W., Lehman, Dawn E., and Berman, Jeffrey W. (2016b) “Experimental Evaluation of the Seismic Vulnerability of Braces and Connections in Older Concentrically Braced Frames,” *Journal of Structural Engineering*, ASCE, DOI: 10.1061/(ASCE)ST.1943-541X.0001507.

Sloat, D. (2014) “Evaluation and Retrofit of Non-Capacity Designed Braced Frames,” a thesis submitted in partial fulfillment of requirements of Master of Science in Civil Engineering, University of Washington, Seattle, WA.

SEAOC (1988) “Recommended Lateral Force Requirements and Tentative Commentary,” Seismology Committee of Structural Engineers Association of California, San Francisco, CA

Terpstra, Clare (2017) “Impact of Beam Strength on Seismic Performance of Chevron Concentrically Braced Frames.” M.S. thesis, University of Washington, Seattle.

Tremblay, R., and Robert, N., (2001) “Seismic performance of low- and medium-rise chevron braced steel frames,” *Canadian Journal of Civil Engineering*, NRC Research Press, Vol. 28, pgs 699-714.

UBC (1994) “Structural Engineering Design Provisions,” *Uniform Building Code Volume 2*, International Conference of Building Officials, Whittier, CA.

Yoo, J-H, Roeder, C.W., and Lehman, D.E (2008). “Analytical Performance Simulation of Special Concentrically Braced Frames,” *Journal of Structural Engineering*, Vol. 134, No 6, pgs 881-889, ASCE, Reston, VA.